ผลของเฟสไทเทเนียและปริมาณทังสเตนที่เติมในตัวเร่งปฏิกิริยา W/TiO_2 ต่อดีไฮเดรชันของเอทานอลเป็นไดเอทิลอีเทอร์

นายพงศธร เกิดน้อย

วิทยานิพนธ์นี้เป็นส่วนหนึ่งของการศึกษาตามหลักสูตรปริญญาวิศวกรรมศาสตรมหาบัณฑิต
สาขาวิชาวิศวกรรมเคมี ภาควิชาวิศวกรรมเคมี
คณะวิศวกรรมศาสตร์ จุฬาลงกรณ์มหาวิทยาลัย
ปีการศึกษา 2560

EFFECTS OF TITANIA PHASE AND TUNGSTEN LOADING CONTENT IN W/TiO_2 CATALYSTS ON DEHYDRATION OF ETHANOL TO DIETHYL ETHER

Mr. Pongsatorn Kerdnoi

A Thesis Submitted in Partial Fulfillment of the Requirements
for the Degree of Master of Engineering Program in Chemical Engineering
Department of Chemical Engineering
Faculty of Engineering
Chulalongkorn University
Academic Year 2017

Thesis Title	EFFECTS OF TITANIA PHASE AND TUNGSTEN LOADING CONTENT IN W/TiO_2 CATALYSTS ON DEHYDRATION OF ETHANOL TO DIETHYL ETHER
By	Mr. Pongsatorn Kerdnoi
Field of Study	Chemical Engineering
Thesis Advisor	Professor Bunjerd Jongsomjit

Accepted by the Faculty of Engineering, Chulalongkorn University in Partial Fulfillment of the Requirements for the Master's Degree

.....Dean of the Faculty of Engineering

(Associate Professor Supot Teachavorasinskun)

THESIS COMMITTEE

.....Chairman

(Professor Muenduen Phisalaphong)

.....Thesis Advisor

(Professor Bunjerd Jongsomjit)

.....Examiner

(Chutimon Satirapipathkul)

.....External Examiner

(Sasiradee Jantasee)

พงศธร เกิดน้อย : ผลของเฟสไทเทเนียและปริมาณทังสเตนที่เติมในตัวเร่งปฏิกิริยา W/TiO_2 ต่อดีไฮเดรชันของเอทานอลเป็นไดเอทิลอีเทอร์ (EFFECTS OF TITANIA PHASE AND TUNGSTEN LOADING CONTENT IN W/TiO_2 CATALYSTS ON DEHYDRATION OF ETHANOL TO DIETHYL ETHER) อ.ที่ปรึกษาวิทยานิพนธ์หลัก: ศ. ดร. บรรเจิด จงสมจิตร , 76 หน้า.

ปัจจุบันเอทานอลซึ่งเป็นพลังงานหมุนเวียนที่ใช้มากที่สุดสามารถเปลี่ยนเป็นสารประกอบที่มีมูลค่ามากขึ้น มีรายงานว่าตัวเร่งปฏิกิริยาทังสเตนบนตัวรองรับไทเทเนีย (W/TiO_2) สามารถเปลี่ยนเอทานอลเป็นไดเอทิลอีเทอร์ได้ อย่างไรก็ตามตัวรองรับไทเทเนียมมีเฟสที่แตกต่างกัน อาจส่งผลต่อสมบัติทางเคมีและกายภาพของตัวเร่งปฏิกิริยาดังนั้นงานวิจัยนี้จึงรายงานถึงพฤติกรรมการเร่งปฏิกิริยาของตัวเร่งปฏิกิริยาที่มีเฟสแตกต่างกันและผลของปริมาณทังสเตนที่เติมต่อดีไฮเดรชันของเอทานอลเป็นไดเอทิลอีเทอร์ ในการเตรียมตัวเร่งปฏิกิริยานี้จะนำตัวรองรับไทเทเนียที่มีเฟสแตกต่างกัน คือ อะนาเทส (A), รูไทล์ (R) และเฟสผสม (P25) มาทำการปรับปรุงด้วยทังสเตนปริมาณ 10 เปอร์เซ็นต์โดยน้ำหนัก และถูกกำหนดเป็น 10W/TiO_2-A, 10W/TiO_2-R และ 10W/TiO_2-P25 ตามลำดับ นอกจากนี้ดีไฮเดรชันของเอทานอลได้ถูกทำการศึกษาเพื่อแสดงประสิทธิภาพในการเร่งปฏิกิริยาของตัวเร่งปฏิกิริยา พบว่าตัวเร่งปฏิกิริยา 10W/TiO_2-P25 ให้ปริมาณการเกิดไดเอทิลอีเทอร์สูงสุด (24.1%) ที่ 300 องศาเซลเซียส และเกิดเอทิลีน (60.3%) ที่ 400 องศาเซลเซียส ในขณะที่ตัวเร่งปฏิกิริยา 10W/TiO_2-R ทำให้เกิด อะซีตัลดีไฮด์เพียง 15.9% เท่านั้น นอกเหนือจากเฟสที่ต่างของตัวรองรับไทเทเนียแล้ว การมีพื้นที่ผิวที่สูงกว่าจะมีบทบาทสำคัญในการกระจายตัวของปริมาณกรดที่ดีขึ้นซึ่งจะนำไปสู่ประสิทธิภาพของการเร่งปฏิกิริยาที่สูงขึ้น ต่อมาตัวรองรับ TiO_2-P25 ถูกเลือกเพื่อศึกษาผลของปริมาณทังสเตนที่เติม (0-20 เปอร์เซ็นต์โดยน้ำหนัก) ซึ่งถูกกำหนดเป็น 5W/TiO_2-P25, 10W/TiO_2-P25, 15W/TiO_2-P25 และ 20W/TiO_2-P25 ตามลำดับ พบว่าตัวเร่งปฏิกิริยา 15W/TiO_2-P25 แสดงประสิทธิภาพในการเร่งปฏิกิริยาสูงที่สุด โดยจะให้ปริมาณไดเอทิลอีเทอร์เท่ากับ 30.4% ที่อุณหภูมิ 300 องศาเซลเซียสและปริมาณเอทิลีนเท่ากับ 65.8% ที่อุณหภูมิ 400 องศาเซลเซียส เนื่องจากบทบาทสำคัญ 3 ประการของตัวเร่งปฏิกิริยาคือ (1) พื้นที่ผิวสูง (2) ปริมาณทังสเตนที่กระจายตัวอยู่บนพื้นผิวด้านนอกของตัวเร่งปฏิกิริยา และ (3) ความเป็นกรดของตัวเร่งปฏิกิริยา ปัจจัยเหล่านี้เป็นปัจจัยที่นำไปสู่การเพิ่มประสิทธิภาพสำหรับดีไฮเดรชันของเอทานอลบนตัวเร่งปฏิกิริยา 15W/TiO_2-P25

ภาควิชา	วิศวกรรมเคมี	ลายมือชื่อนิสิต .....
สาขาวิชา	วิศวกรรมเคมี	ลายมือชื่อ อ.ที่ปรึกษาหลัก .....
ปีการศึกษา	2560	

5970251921 : MAJOR CHEMICAL ENGINEERING
KEYWORDS: ETHANOL DEHYDRATION, TITANIA, TUNGSTEN, DIETHYL ETHER, ETHYLENE

PONGSATORN KERDNOI: EFFECTS OF TITANIA PHASE AND TUNGSTEN LOADING CONTENT IN W/TiO_2 CATALYSTS ON DEHYDRATION OF ETHANOL TO DIETHYL ETHER. ADVISOR: PROF. BUNJERD JONGSOMJIT, 76 pp.

Nowadays, ethanol which is one of the most used renewable energies can be converted into the more valuable compounds. It was reported that titania-supported tungsten (W/TiO_2) catalyst is able to convert ethanol into diethyl ether. However, titania support has different crystalline phases that can result in differences of physicochemical properties for the catalyst. Therefore, the present work reports on the catalytic behaviors of both different phases of titania and tungsten loading contents in catalytic ethanol dehydration to diethyl ether. To prepare the catalysts, the three different phases [anatase (A), rutile (R), and mixed phases (P25)] of titania supports were impregnated with 10 wt% of tungsten and denoted as 10W/TiO_2-A, 10W/TiO_2-R, and 10W/TiO_2-P25, respectively. Moreover, ethanol dehydration was also performed to determine the overall activities for all catalysts. It was found that the 10W/TiO_2-P25 catalyst exhibits the highest DEE yield (24.1%) at 300°C and ethylene yield (60.3%) at 400°C, whereas only 15.9% is obtained from 10W/TiO_2-R catalyst. Besides the different phases of titania support, higher surface area of TiO_2 is likely to play an important role on the better dispersion of acid sites leading to higher catalytic activity. Moreover, TiO_2-P25 support was selected to further study to investigate the effect of W loading (0-20 wt%), which was denoted as 5W/TiO_2-P25, 10W/TiO_2-P25, 15W/TiO_2-P25 and 20W/TiO_2-P25, respectively. It was found that the 15W/TiO_2-P25 catalyst gives the highest activity with DEE of 30.4% yield at 300°C and ethylene of 65.8% yield at 400°C due to its three major roles including; (1) high surface area, (2) high amount of W species distributed on the external surface of catalyst and (3) introduce acid sites as active sites in the reaction. There were the factors leading to obtain higher activity for ethanol dehydration of 15W/TiO_2-P25 catalyst.

Department: Chemical Engineering Student's Signature .....
Field of Study: Chemical Engineering Advisor's Signature .....
Academic Year: 2017

ACKNOWLEDGEMENTS

The author would like to express the deepest gratitude to his thesis advisor, Professor Bunjerd Jongsomjit, not only for his professional guidance and support for solving problems throughout this research, but also for his indefatigable patience and encouragement whenever the author had a rough time in the research. His wisdom, knowledge and commitment to the highest standards always inspired and motivated him.

In addition, the author is also thankful for chairman of the committee, Professor Muenduen Phisalaphong and members of the thesis committee, Chutimon Satirapipathkul and Sasiradee Jantasee for their dedicated in taking valuable time for his research suggestions.

Furthermore, the author would like to thank for the Grant for International Research Integration: Chula Research Scholar, Ratchadaphiseksomphot Endowment Fund and Grant for Research: Government Budget, Chulalongkorn University (2018) for financial support of this research.

Most of all, the author owes so much to his family who were always there standing by him and encouraging him with love, understanding and patience in the good times and bad. The author would like to express the gratefully acknowledge to his co-worker and friends in Center of Excellence on Catalysis and Catalytic Reaction Engineering and others for being a companion with him throughout the joyful and tough times.

CONTENTS

Page

Page

Page

FIGURE CONTENTS

TABLE CONTENTS

CHAPTER 1
INTRODUCTION

1.1 Introduction

Currently, renewable energy resources such as solar, wind and biomass have become an important way to achieve sustainable development. Increasing renewable energy consumption in the world can impact on the utilization of fossil fuel that is finite resources. One of the most used renewable energies is ethanol, which can be derived from fermentation of various types of agricultural products such as sugarcane, cassava, molasses, rice, corn, and millet [1].

In fact, ethanol can be converted into various valuable chemical compounds including ethylene and diethyl ether (DEE) via dehydration and acetaldehyde via dehydrogenation of ethanol [2].

$$C_2H_5OH \longrightarrow C_2H_4 + H_2O \qquad \Delta H_{298} = +44.9 \text{ kJ/mol} \qquad (1)$$

$$2C_2H_5OH \longrightarrow C_2H_5OC_2H_5 + H_2O \qquad \Delta H_{298} = -25.1 \text{ kJ/mol} \qquad (2)$$

$$C_2H_5OH \longrightarrow C_2H_4O + H_2 \qquad \Delta H_{298} = +69.1 \text{ kJ/mol} \qquad (3)$$

Reaction (1) and (2) are two competitive routes for dehydration of ethanol as endothermic reaction and exothermic reaction, respectively. Thus, the formation of ethylene favors at high temperature (400-450°C) to obtain high ethylene selectivity, while DEE mainly occurs at low temperature (<300°C). Ethylene product is widely used as raw materials in the manufacture of various polymers such as polyethylene, polyvinyl chloride, and polystyrene and other organic chemicals [3]. The DEE product is commonly used as an extraction solvent. Moreover, DEE has high cetane number and can be used in combination of petroleum fuel for gasoline and diesel engines [4, 5]. In addition, for the endothermic reaction of ethanol dehydrogenation, acetaldehyde that is an important raw material in the production of many chemical products can be formed as a byproduct [5, 6].

It is well known that the catalytic dehydration of ethanol has been investigated using different catalysts in order to increase activity and lower the operation temperature. Normally, the solid acid catalysts containing alumina (Al_2O_3) and

transition metal oxides such as zeolite, montmorillonite clays, silica (SiO_2), zirconia (ZrO_2), and titania (TiO_2) are employed. However, they are presently expanded to include many catalysts, which are modified by adding other metals [7, 8]. Among noble and transition metals, tungsten (W) is the most interesting choice since it is widely used. Moreover, W is an acidic catalytic material being highly active and selective for many reactions [9]. It was revealed that the addition of W onto titania support gave higher activity at the low temperature due to increased strong Brønsted acid sites for catalytic reaction [10]. Regarding the catalyst supports, it is recognized that titania exists in three different crystalline phases including anatase, brookite, and rutile. Anatase usually exhibits better activity than that of brookite and rutile. However, there are several reactions for the unexpectedly high activity of brookite and rutile [11-13]. Therefore, the different compositions of crystalline phases could exhibit the different physicochemical properties of titania.

In this proposed research, W/TiO_2 catalysts were prepared by using titania supports having different phase compositions. All catalysts were characterized by using various characterization techniques including Inductively coupled plasma (ICP), X-ray diffraction (XRD), scanning electron microscope (SEM) and electron dispersive X-ray (EDX) spectroscopy, N_2-physisorption, Temperature-programed desorption of ammonia (NH_3-TPD) and Thermal gravimetric analysis (TGA). Furthermore, the catalysts were tested in ethanol dehydration reaction under vapor phase of ethanol. To understand the catalytic behaviors of different titania phases, the effect of phase compositions in titania supports on the catalytic properties and product distribution were elucidated and discussed. Besides, the effect of W loading in catalysts were also investgated in the similar way.

1.2 Motivation

Ethanol dehydration is very interesting reaction in order to convert agricultural product, ethanol, into the more valuable compounds. It was reported that titania-supported tungsten (W/TiO_2) catalyst is one of suitable catalysts for the reaction.

1.3 Research objectives

1) To investigate the changes in catalytic behaviors with different phases of titania as a support for tungsten catalyst in ethanol dehydration.
2) To compare the effect of tungsten loading onto titania support for ethanol dehydration.

1.4 Research scopes

1) W/TiO_2 catalysts were prepared by incipient wetness impregnation.
2) A 10 wt% of tungsten were impregnated onto the titania supports: anatase (A), rutile (R), and mixed phases (P25)
3) The tungsten contents (5, 10, 15 and 20 wt%) were varied and impregnated onto the titania support giving the highest DEE yield.
4) The obtained catalysts were characterized by using ICP, XRD, SEM/EDX, N_2-physisorption, NH_3-TPD, and TGA.
5) The ethanol reactions were preformed under atmospheric pressure and temperature between 200 to 400°C.
6) All products were analyzed by gas chromatography (GC) with FID.

1.5 Expected benefits

1) The W/TiO_2 catalysts for ethanol dehydration have been improved.
2) It can obtain the suitable catalyst to produce DEE via ethanol dehydration.
3) It will be an alternative route for catalytic dehydration of ethanol
4) It can be applied for future ethanol industries in Thailand

CHAPTER 2

THEORY AND LITERATURE REVIEWS

2.1 Ethanol

Ethanol (ethyl alcohol) is manufactured by the fermentation of a wide variety of agricultural materials. Ethanol is one of the most promising and alternatives to fossil fuels, which use as an additive in gasoline.

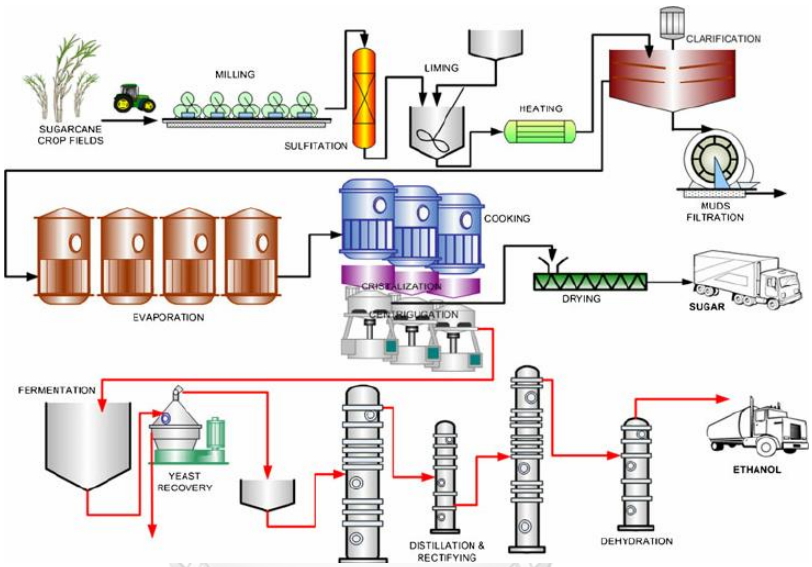

Figure 1 Productive system to produce ethanol from sugarcane [14]

2.2 Ethanol dehydration

Ethanol dehydration is an example of elimination reaction. Dehydration of alcohol follows two competitive routes to produce; (1) ethylene via an endothermic reaction at high temperature, and (2) diethyl ether via an exothermic reaction at lower temperature. Ethylene product is widely used as raw materials in the manufacture of various polymers such as polyethylene, polyvinyl chloride, and polystyrene and other organic chemicals [3]. The DEE product is commonly used as an extraction solvent. Moreover, DEE has high cetane number and can be used in combination of petroleum fuel for gasoline and diesel engines [4, 5].

For ethylene production, reaction is suggested to occur through E2 elimination route, which is concerted break bonds of C-H and C-O in ethanol using a pair of Brønsted acid (OH) and base (B) catalyst sites. Then, ethylene and water are produced after this step (**Figure 2**).

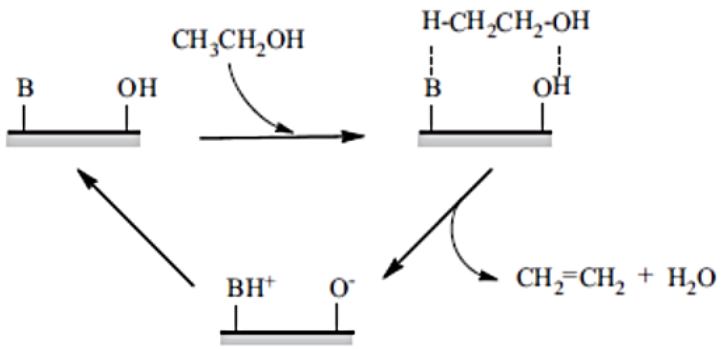

Figure 2 The formation of ethylene via E2 elimination of ethanol [4]

Diethyl ether (DEE) is formed by two different pathways, associative pathway and dissociative pathways (**Figure 3**). Both pathways are supposed to take place at Brønsted acid sites (OH). The dissociative (stepwise) pathway is explained by initial ethanol adsorption, followed by water elimination from ethanol, leading to adsorbed ethyl and water. After that, ethyl group reacts with the other ethanol molecule to form diethyl ether. The associative (direct) pathway is explained by co-adsorption of two ethanol molecules, which react and form the ether directly.

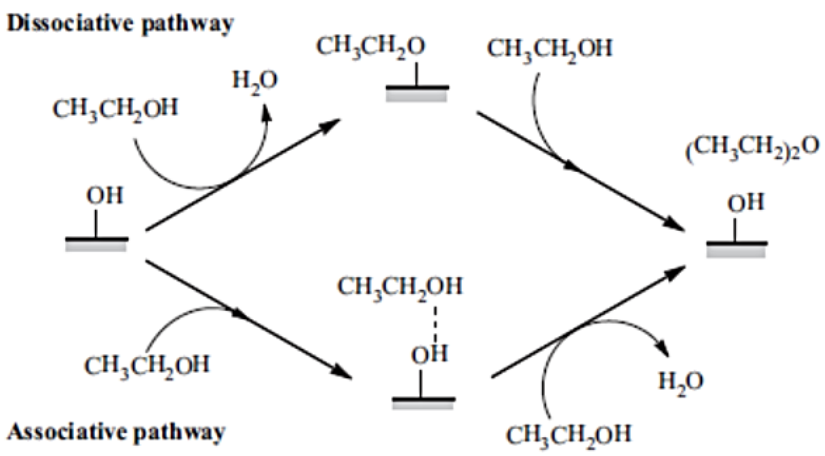

Figure 3 Associative and dissociative pathways for diethyl ether formation [4]

2.3 Catalysts

A catalyst is used to change the reaction kinetics of a reaction and decrease the activation energy, which is needed for a reaction to occur. It can speed up a reaction toward the equilibrium but cannot change the equilibrium of a reaction. The catalyst is not consumed during the reaction but it can be deactivated and loose its ability to catalyze the wanted reaction. There are some concepts that are important when talking about catalysts. The catalytic concepts in focus are activity, selectivity and deactivation. The activity is a measurement of how fast the reaction reaches the equilibrium. Selectivity describes the capability to produce a desired product. Deactivation is when a catalyst loses its ability to catalyze a reaction and becomes less active.

Heterogeneous catalysts can be widely used for the dehydration of ethanol. A heterogeneous catalyst consists of three parts, these are carrier, support and active site. The carrier provides structure to the catalyst and the reactor bed; it determines the heat and mass transfer properties and also governs the pressure drop over the reactor. The support provides surface area, on which the reaction can occur, and can be of the same material as the carrier. The surface area of the support is important since this is where the active sites are dispersed. The active sites are where the reaction actually occurs and can be the material of the support. Some common materials are alumina, silica and mixed oxides [15, 16].

2.4 Tungsten (VI) oxide (WO_3)

Tungsten (VI) oxide is a chemical compound containing tungsten metal and oxygen with the chemical formula WO_3. Tungsten trioxide has many crystal structures depended on temperature. There are tetragonal (above 740°C), orthorhombic (330-740°C), and monoclinic (17-330°C). Therefore, the monoclinic is stable at room temperature, and the tetragonal is stable at high temperatures and often found in the form of elongated particles with high aspect ratios [17].

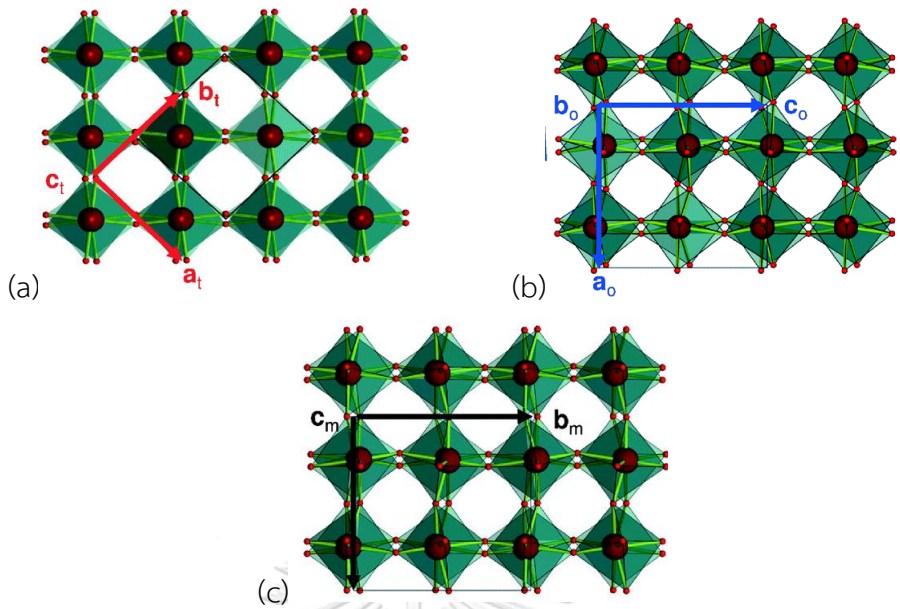

Figure 4 The three crystal phases of tungsten oxide
(a) tetragonal, (b) orthorhombic, and (c) monoclinic. [18]

It is extensively used for many purposes with applications in heterogeneous catalysis, photocatalysis, electronic devices, and corrosion protection. In catalytic field, it was presented that tungsten oxide mixed with other oxides are primarily active for isomerization of alkanes and alkenes, metathesis of alkenes, partial oxidation of alcohols, and selective reduction of NO_x [19].

2.5 Titanium (IV) oxide (TiO_2)

Titanium (IV) oxide, which is also known as titania or TiO_2, has three different crystal structures: anatase (tetragonal), rutile (tetragonal) and brookite (orthorhombic). Rutile is the most stable form of titania. Anatase and brookite are stable at normal temperatures but slowly convert to rutile upon heating to temperature above 550 and 750°C, respectively. All three forms of titania have six coordinated titanium atoms in their repeating unit cells. Both rutile (**Figure 5 (a)**) and anatase (**Figure 5 (b)**) structures are tetragonal. The anatase unit cell is more elongated, while rutile unit cells occupy the least space. This makes the rutile form the most stable at higher temperatures.

The distortion is greatest in brookite (**Figure 5 (c)**), the least stable and least common crystal structure [20, 21].

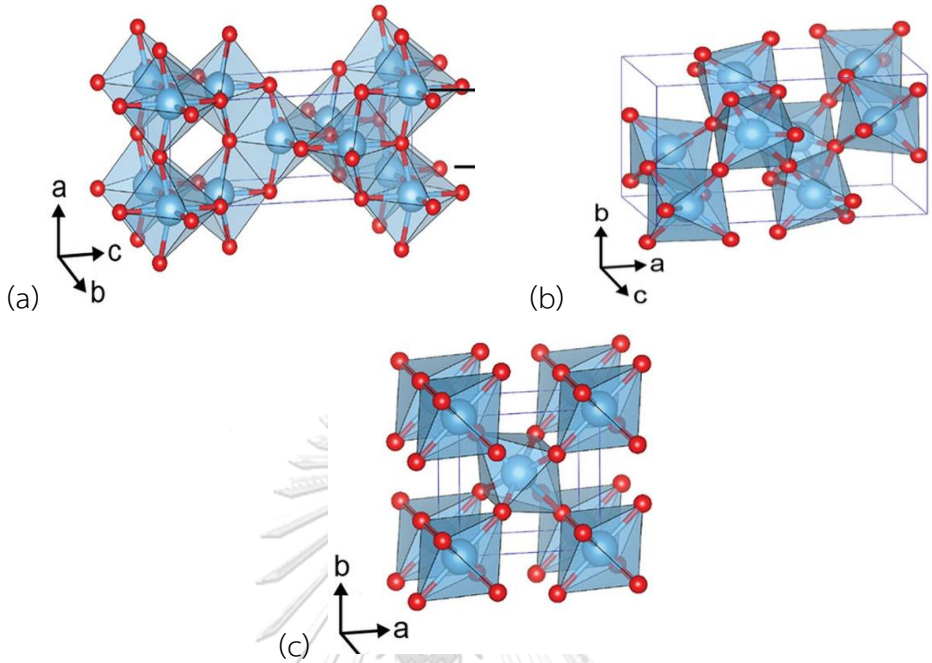

Figure 5 Crystal structures of TiO_2 (a) anatase, (b) brookite and (c) rutile The titanium atoms are shown in blue, the oxygen atoms in red. [22]

Moreover, manufacturers produce nano-structured titania with good properties and particle size around 25 nm as called TiO_2-P25, which contains a mixture of anatase and rutile in an approximately 3:1 proportion.

To increase the activity, TiO_2 can be modified in different ways, for example by adding oxides like MgO/SiO_2, Cr_2O_3, FeO_x and TiO_2. There are numerous of other ways to improve the oxide catalysts and thus increase the ethanol conversion and selectivity. One of the problems with this type of catalyst is the high reaction temperature required. Another problem is that water can deactivate active sites on **γ**-Al_2O_3 and inhibit the formation rate of ethylene and diethyl ether [8, 16].

High surface area anatase is widely used as support of catalysts. We also know that anatase can transform into rutile when its use for high-temperature reactions. Anatase may offer good opportunity for relatively low-temperature reaction (<400°C). One of the most important applications of titania in field of heterogeneous catalysis is as the support for metal catalysts such as, e.g., vanadium, tungsten, and molybdenium.

A particular effect has been object of many studies, such as the SMSI effect (Strong Metal Support Interaction), occurring when transition metal oxides are used as supports under reducing conditions and at elevated temperatures. Rutile seems to have less interest as catalyst support. However, it is a stable phase thus allowing higher temperature applications. Some companies brought a rutile-supported RuO_2 catalyst for the catalytic oxidation of HCl to Cl_2.

2.6 Incipient wetness impregnation

Incipient wetness impregnation (IWI) is a normally used technique for the preparation of heterogeneous catalysts. The active metal precursor is dissolved in an aqueous solution. Then the obtained solution is slowly dropped to a particle as support containing the same pore volume as the volume of the added solution. Capillary action draws the solution into the pores. Solution added in excess of the support pore volume causes the solution transport to change from a capillary action process to a diffusion process, which is much slower. After that, the catalyst was dried and calcined to eliminate the impurities in the solution [23].

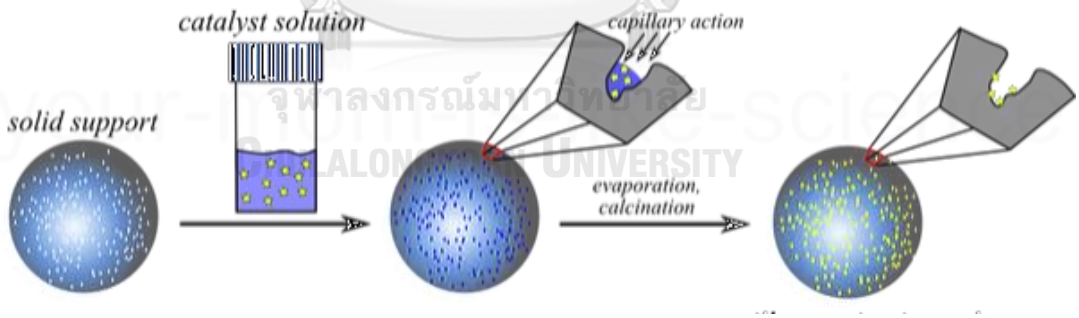

Figure 6 Steps of the incipient wetness impregnation [24]

2.7 Literature reviews

Nowadays, fossil fuel provides about 85% of all the energy used in the world. The major reason of rapid reducing petroleum reserve is high consumption rate that cause major environmental problems such as emission of CO_2 and harmful emissions. It is important to find alternative fuels. Ethanol, ethyl alcohol, is one of the most used

renewable energy that is a good option and may facilitate the reduction of CO_2 and harmful gases. Ethanol has been derived from agricultural products; sugarcane, cassava, molasses, rice, corn, millet, and algae [1].

Ethanol can be converted into various valuable compounds by dehydration and dehydrogenation of ethanol. Ethanol dehydration has been of interest to produce; (1) ethylene via an endothermic reaction (400-450°C) with the decomposition of ethoxy groups over catalysts and (2) diethyl ether (DEE) via an exothermic reaction (<300°C) with the reaction of ethoxy groups with undissociated ethanol. Moreover, acetaldehyde can be produced by endothermic reaction of ethanol dehydrogenation [4, 25-27].

It is well known that the catalytic dehydration of ethanol has been investigated different solid acid catalysts to increase productivity and lower reaction temperature. Normally, the catalysts began with alumina, silica and transition metal oxides [6, 7, 28]. However, these catalysts are modified by loading other metals for improving the catalytic activity. Several workers reported that increased metal loading and acid density in catalysts resulted in increased weak Brøndsted acid sites leading to improve catalytic activity of ethanol dehydration reaction. Therefore, the most factor affecting the catalytic activities is the acidity, which depended on the presence of metal loading [29-32].

Among noble and transition metals, tungsten (W) is the most interesting choice for applications in the chemical industries. The supported tungsten oxide catalysts are used for a large number of industrial reactions, such as the selective catalytic reduction of NO_x, isomerization of alkanes and alkenes, the metathesis of alkenes, photocatalytic reactions and the conversion of alcohols [33, 34].

During the past decades, it has been shown that tungsten oxides were mixed with other oxides to increase the catalytic activity. In the field of ethanol dehydration, Phung et al. [10] reported that tungsten oxide supported by titanium dioxide is able to convert ethanol into diethyl ether, which is higher valuable than raw material. The addition of WO_3 to TiO_2 is widely used for acid catalyst due to introduce Brønsted acid sites that are supposed to represent the active sites in the reaction, but also prevents the formation of byproducts, i.e. acetaldehyde and higher hydrocarbons due to

poisoning of basic sites and of reducible surface Ti center. Normally, the WO_3/TiO_2 catalysts are prepared by impregnation method from the precursor of ammonium metatungstate. However, there are many methods to prepare this catalyst, such as by physical mixing, coprecipitation and sol-gel method [35]. It should be noted that tungsten oxide species can be present in two forms as monotungstate and polytungstate species. Ladera et al. [36] recognized that tungsten oxides are highly dispersed on TiO_2 as monotungstate species at low W surface densities (up to 2.3 at. W nm^{-2}). Otherwise, higher W surface densities display the formation of polytungstates until complete monolayer surface coverages. Previously, Onfroy et al. [9, 37] studied the acidity of catalyst systems based on tungsten oxide supported on titania for isopropanol dehydration. At reaction temperature of 403 K, the activity is very low until W loading up to 1.2 at. W nm^{-2}. Above this loading, the catalysts were progressively active with increasing W loading. It is because polytungstate species were formed and these are responsible for the observed Brønsted acid sites. Moreover, in 1999, Sohn and Bae [38] described the characterization of tungsten oxide supported on titania. The result showed that the presence of WO_3 strongly influences the textural properties. The surface area and acidity of catalysts increase in proportion to the WO_3 content up to 20 wt%. It can conclude that the molecular structure of tungsten oxide species and their acid property are obviously influenced by the W surface density, which also related to the catalytic activity [39].

Commonly, Titania has three polymorphous phases: anatase, brookite and rutile. These phases exhibit different properties and consequently different catalytic performances. Generally, titania has a surface area of ~50 m^2/g. However, it depends on the method of synthesis as well as precursors that we used during synthesization [40]. In terms of applications, anatase is more preferable as it is generally more stable compared to rutile phase. However, the combination of anatase and rutile lead to a synergetic effect between two phases that improves the catalytic activity of TiO_2 [41]. To clarify the crystalline phase effect of TiO_2 supports, Jongsomjit et al. [11, 12] studied the effect of cobalt dispersion on titania consisting various rutile:anatase ratios. It was proposed that the increased number of reduced cobalt metal surface atom can be attributed to highly dispersed cobalt oxide species. Moreover, the presence of rutile

phase in TiO_2 support could facilitate the reduction of highly dispersed cobalt oxide species into the reduced cobalt metal surface atoms, which is related to the activity in CO hydrogenation. In addition to confirm the results, Yao et al. [42] synthesized a series of anatase, brookite, and rutile, and then used as supports to prepare the supported ceria-based catalysts for NH_3-SCR. The obtained results showed that cerium oxide species are highly dispersed on the surface of TiO_2 supports and strongly interacts with these TiO_2 supports. Besides, the interaction between CeO_2 and TiO_2 depends on the crystal form of TiO_2 and probably leads to the amounts of acid sites and surface Ce^{3+} contents. Furthermore, Rui at al. [43] found that the strong-metal-support-interaction (SMSI) in mixed phases TiO_2 supported Pt catalysts is stronger than single phase TiO_2 supported Pt. Owing to its high interaction, Raj and Viswanathan [44] studied the catalytic properties of P25 titania, contains anatase and rutile phases in a ratio of about 3:1, on the phase transformation of anatase to rutile using different calcined temperatures. It was reported that P25 tatinia samples can be used for the reaction temperature lower than 500 °C due to prevent a complete conversion from anatase to rutile and decrease the surface area and pore volume. Therefore, the different phases of titania can affect the catalytic properties and catalytic activity

CHAPTER 3

EXPERIMENTAL

3.1 Research methodology

Part I : The characteristic and catalytic activity of W/TiO_2 catalysts with different phases of TiO_2 (anatase, rutile, and P25)

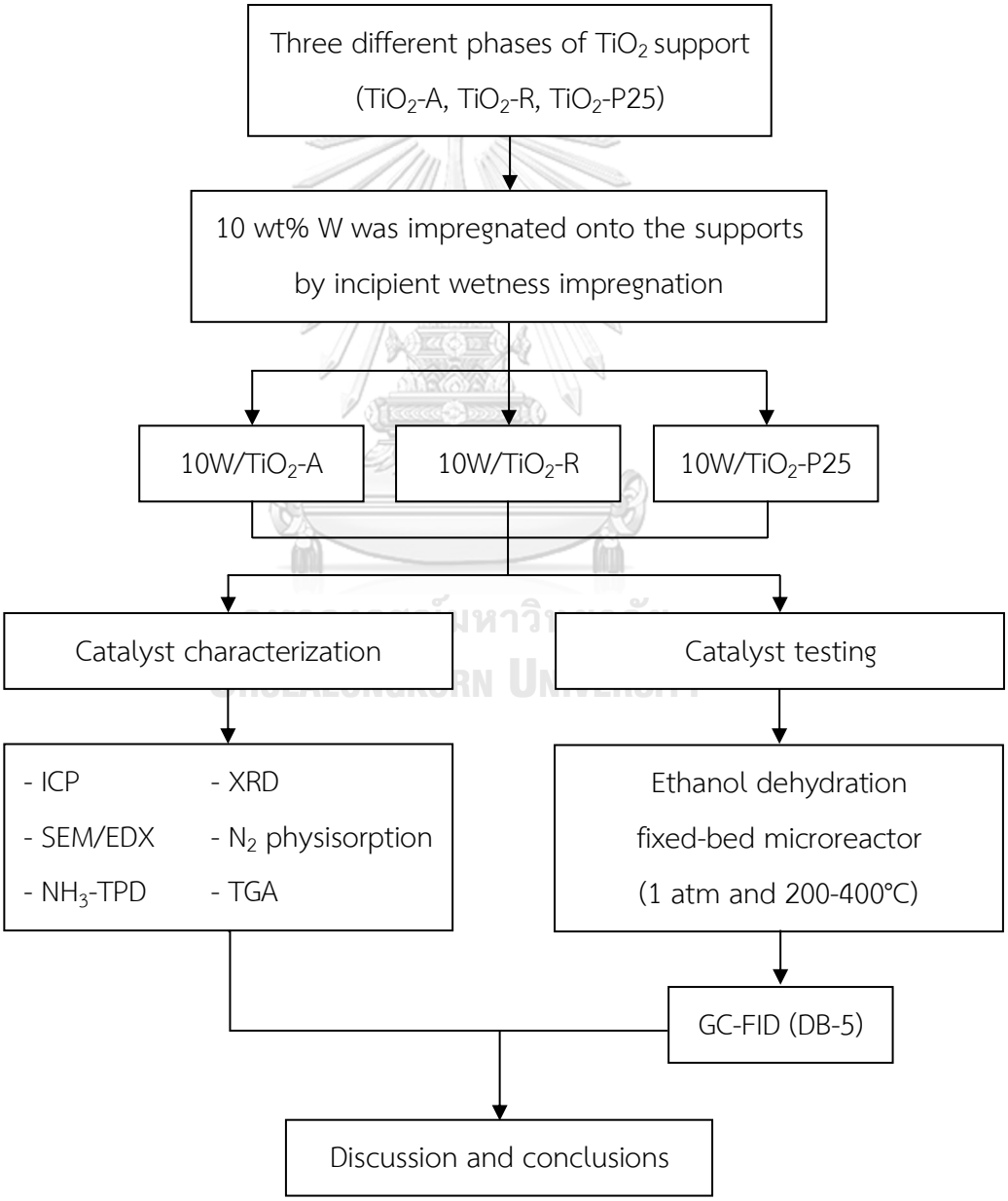

Part II : The characteristic and catalytic activity of W/TiO_2-P25 catalysts with different loading of tungsten (0-20 wt% W)

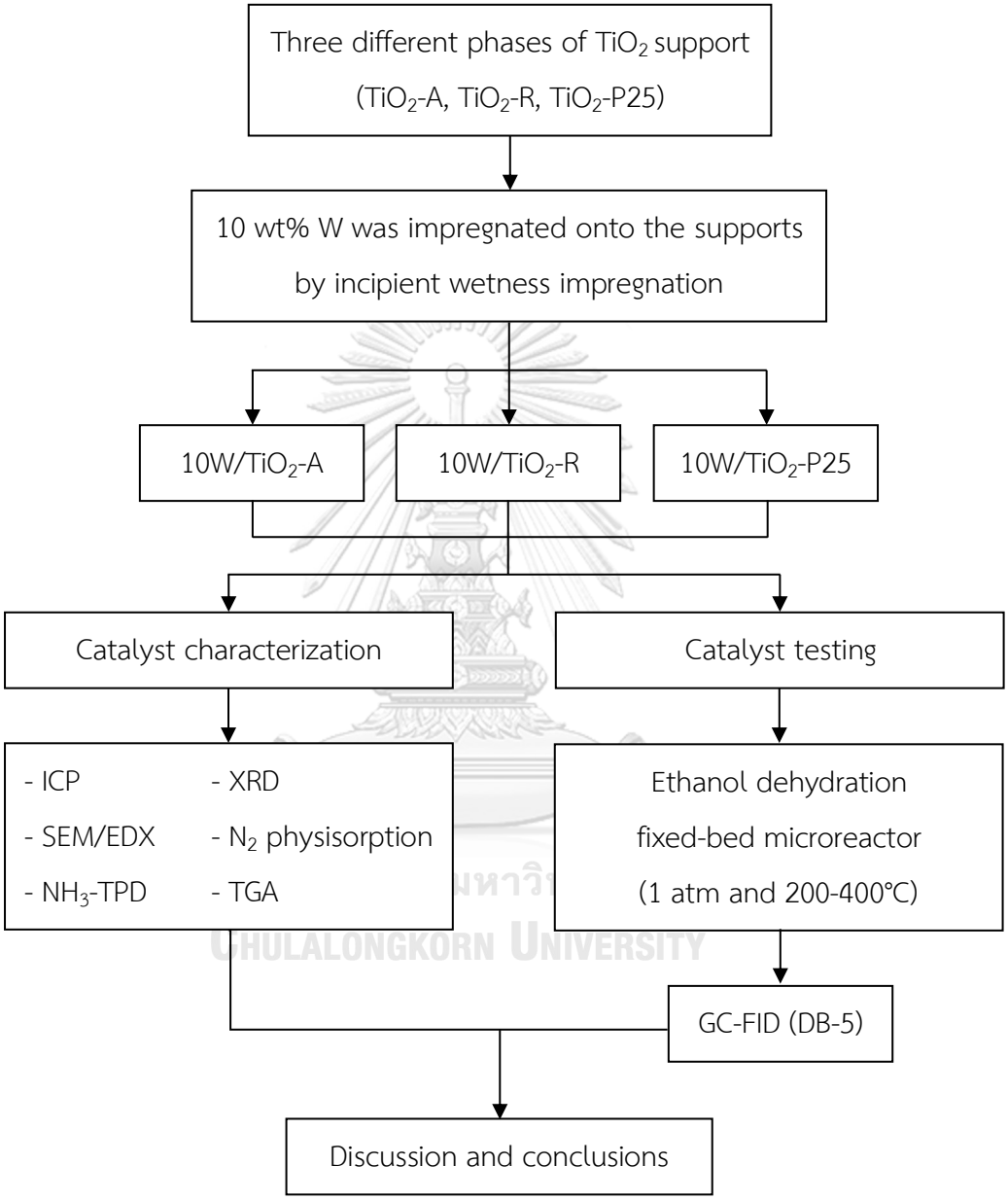

3.2 Catalyst preparation

3.2.1 Chemicals

- Titanium (IV) oxide or titania (TiO_2): anatase, rutile and P25 from Sigma-Aldrich
- Ammonium metatungstate ($(NH_4)_6H_2W_{12}O_{40} \bullet 4H_2O$) from Sigma-Aldrich
- Ethanol (C_2H_5OH) 99.99% from VWR
- Ammonia (NH_3) from Panreac
- De-ionized water

3.2.2 Preparation of W/TiO_2 catalysts with different phases

A tungsten content of 10 wt% was prepared by incipient wetness impregnation onto the TiO_2-A, TiO_2-R, and TiO_2-P25 supports with an aqueous solution of ammonium metatungstate. After impregnation, the catalyst samples were dried at 110°C for 24 h and then calcined in air at 500°C for 3 h.

3.2.3 Preparation of W/TiO_2 catalysts with different W loading

The phase of titania giving the highest activity was selected to further study on the effect of tungsten loading content for ethanol dehydration. These catalysts were prepared prior to the method.

3.2.3 Catalysts nomenclature

The nomenclature used for the catalysts in this study is as follows:

XW/TiO_2-Y : X refers to tungsten loading content of XX wt%

: Y refers to titania phase composed of anatase (A), rutile (R), and mixed phases (P25).

3.3 Catalyst characterization

3.3.1 Inductively coupled plasma (ICP)

A quantity of elemental composition in the catalysts was measured by Perkin Elmer OPTIMA2000^{TM} instrument. Before testing, sample must be converted to liquid form before testing by dissolving the sample in a solvent (typically acid) to produce a solution.

3.3.2 X-ray diffraction (XRD)

The crystalline phases were identified using a SIEMENS D-5000 X-ray diffractometer with Cu K_α (λ= 1.54439 Å). The pattern was recorded over the 2θ between 20° and 80°.

3.3.3 Scanning electron microscope (SEM) and energy dispersive X-ray spectroscopy (EDX)

The simple morphologies and elemental distribution were respectively examined by SEM using a JEOL JSM-5800LV model and EDX using Link Isis series 300 program. Before analysis, all samples were dried at 110°C for 24 h.

3.3.4 N_2 physisorption

The adsorption-desorption isotherms of nitrogen at -196°C were obtained from adsorptiometer (Micromeritics ASAP 2010). The specific surface areas were determined from adsorption values for relative pressure (P/P_0) by using the BET method. The total pore volume was estimated from the total amount of adsorbed nitrogen by using the BJH method. All samples were vaporized moisture before the analysis.

3.3.5 Ammonia temperature-programmed desorption (NH_3-TPD)

The acid properties of obtained catalysts were investigated by NH_3-TPD using Micromeritics Chemisorp 2750 Pulse Chemisorption System. 0.05 g of catalyst was packed on quartz wool in a glass tube and pretreated at 550°C under with 10°C/min.

After cooled temperature at 40°C, the catalyst was saturated with 15% NH_3 for 30 minutes and heated to 550°C with 10°C/min in order to desorp NH_3.

3.3.6 Thermal gravimetric analysis (TGA)

The thermal decomposition of titania-supported catalyst was studied by thermal gravimetric analysis under the temperature range of room temperature to 1000 °C with a heating rate of 10 °C/min in nitrogen atmosphere using a STD analyzer model Q600 from TA instrument.

3.4 Reaction study of ethanol dehydration

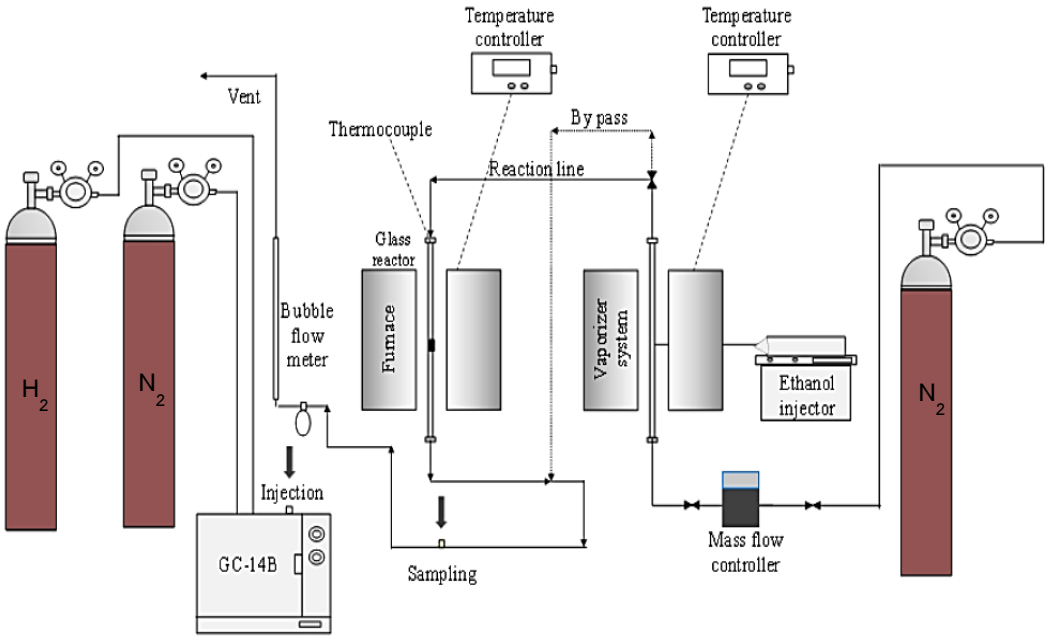

Figure 7 Experimental set-up for reaction test

The catalytic ethanol dehydration was performed at the fixed-bed microreactor and the experimental set-up apparatus as show in **Figure 7**.

3.4.2.1 Temperature controller

The temperature controller is used to control three parts in the experimental apparatus; furnace (200–400°C), vaporizer, and heating tape.

3.4.2.2 Mass flow controller

Nitrogen is used as a carrier gas and its flow rate controlled by mass flow controller.

3.4.2.3 Syringe pump

The syringe pump is used to feed ethanol into vaporizer at rate of 1.45 ml/h.

3.4.2.4 Vaporizer

The vaporizer is used to vaporize liquid ethanol to vapor phase. It is operated at atmospheric pressure and temperature of 120°C for vaporized ethanol.

3.4.2.5 Reactor

The fixed-bed microreactor is made from glass tube with an inside diameter of 7 mm and length of 330 mm

3.4.2.6 Furnace

The furnace is used to heat the catalyst in a reactor tube.

3.4.2.7 Heating tape

The heating tape is covered on the pipeline to prevent the condensation of product.

3.4.2.8 Sampling port

The obtained products are collected at sampling port with 1.0 ml to analyze by GC-FID.

3.4.2.9 Gas chromatography

A gas chromatography is used to investigate ethanol conversion and product selectivity (ethylene, diethyl ether, and acetaldehyde). It equipped with flame ionization detector (FID) with DB-5 capillary column. Nitrogen (99.99 vol%) and Hydrogen (99.99 vol%) are used as carrier gas. The temperature of initial column, final column, injector, and detector are 40, 40, 150, and 150°C, respectively.

3.5 Reaction test

The catalytic ethanol dehydration was performed under atmospheric pressure in a fixed-bed microreactor. The catalyst (0.05 g) was charged onto packed quartz wool (0.01 g) in the middle of microreactor. In order to eliminate the impurity on surface of catalyst prior to reaction, the catalyst was pretreated in nitrogen with 60 ml/min at 200°C for 1 h. Then, ethanol was vaporized and fed with controlled by a single syringe pump with at total flow rate of 1.45 ml/h (22.9 h^{-1} WHSV). Finally, all products were collected and analyzed at temperatures of 200, 250, 300, 350, and 400°C by GC-FID.

3.7 Research plan

Table 1 Schedule of the research plan

Research plan	2017									2018					
	Apr	May	Jun	Jul	Aug	Sep	Oct	Nov	Dec	Jan	Feb	Mar	Apr	May	Jun
Studied about the theory related to ethanol dehydration reaction and their catalysts.	←	—	—	—	—	→									
Considered the variables associated with the research.		←	—	→											
Prepared 10W/TiO_2 catalysts with different phases of titania (A, R and P25).				←	—	→									
Characterized all supports and 10W/TiO_2 catalysts with different phases of titania.					←	—	—	—	→						
Studied the catalytic activities via ethanol dehydration reaction.						←	—	—	—	→					
Prepared W/TiO_2-P25 catalysts with different W loading (5, 15 and 20 wt%).								←	—	→					
Characterized all W/TiO_2-P25catalysts with different W loading.									←	—	—	—	→		
Studied the catalytic activities via ethanol dehydration reaction.										←	—	—	—	→	
Analyzed, discussed and concluded the obtained results.							←	—	—	—	—	—	—	→	
Prepared the report for presentation.														←	→

CHAPTER 4
RESULTS AND DISCUSSION

In this chapter, the results and discussion of W/TiO_2 catalysts are described on characteristics and catalytic activities. All catalysts were prepared by incipient wetness impregnation as mentioned in chapter 3 and studied in ethanol dehydration reaction under vapor phase of ethanol at temperature range between 200°C and 400°C. All catalysts were characterized by using various characterization techniques including inductively coupled plasma (ICP), X-ray diffraction (XRD), scanning electron microscope (SEM) and electron dispersive X-ray (EDX) spectroscopy, N_2-physisorption, temperature-programed desorption of ammonia (NH_3-TPD) and thermal gravimetric analysis (TGA). The results and discussion are divided into 3 parts. The first part decribes the charateristics and catalytic activity of W/TiO_2 catalysts with different pahses of TiO_2. The second part describes the characteristic and catalytic activity of W/TiO_2-P25 catalysts with different loading of tungsten (0-20 wt% W). The final part shows the comparison of catalysts for DEE synthesis and their catalytic activity.

Part I : The characteristic and catalytic activity of W/TiO_2 catalysts with different phases of TiO_2 (anatase, rutile, and P25)

W/TiO_2 catalysts were prepared by incipient wetness impregnation of 10 wt% tungsten onto titania supports having different phase compositions and then studied both catalytic properties and performance in ethanol dehydration.

4.1.1 Inductively coupled plasma (ICP)

Three different phase compositions of TiO_2 including anatase (A), rutile (R) and mixed phases (P25) were modified with tungsten (W) by incipient wetness impregnation. The supports and obtained catalysts with different phase compositions were taken to determine the composition and amount of element in bulk catalyst by inductively coupled plasma (ICP) as shown in **Table 2**.

Table 2 The amount of tungsten contained in bulk catalysts

Catalysts	Amount of W in bulk catalysts (wt%)
10W/TiO_2-A	10.66
10W/TiO_2-R	10.11
10W/TiO_2-P25	10.22

The amount of W content is named following ICP result. Therefore, the nomenclature of catalysts having different phase (anatase, rutile and P25) of titania in this part are denoted as 10W/TiO_2-A, 10W/TiO_2-R and 10W/TiO_2-P25, respectively.

4.1.2 X-ray diffraction (XRD)

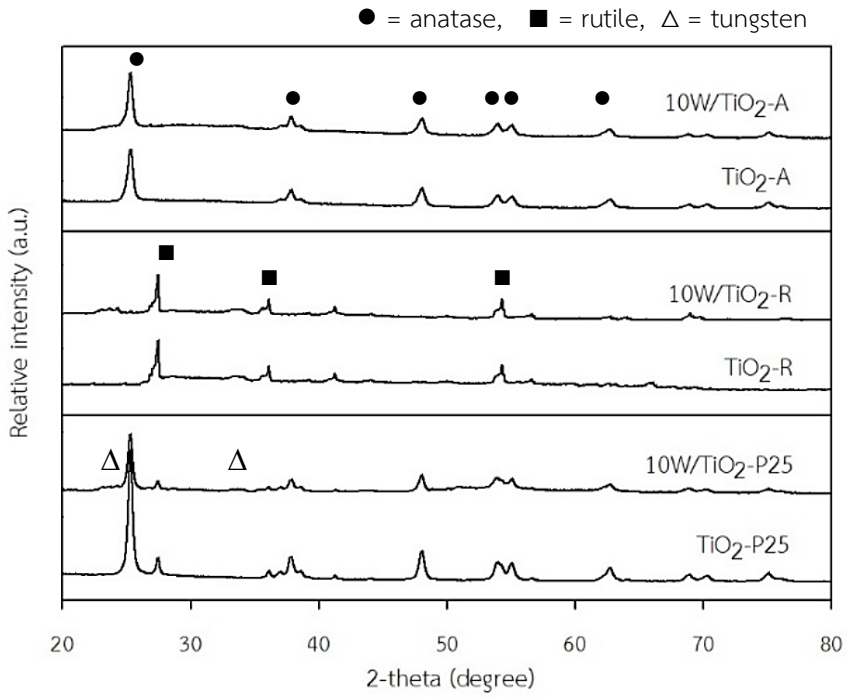

Figure 8 XRD patterns of supports and catalysts with different phase of TiO_2

To identify the crystalline structure of the catalysts after W doping, the X-ray diffraction (XRD) was performed. The XRD patterns of TiO_2 supports and 10W/TiO_2 catalysts are illustrated in **Figure 8**. Results show that TiO_2-A support displays the anatase peaks at 25° (major), 37, 48, 54, 55 and 62°, whereas TiO_2-R support exhibits rutile peaks at 27° (major), 36° and 55° [12]. Moreover, TiO_2-P25 support, which contains a mixture of anatase and rutile in an approximately 3:1 proportion, demonstrates both peaks of titania anatase and rutile phase. The 10 wt% of W was impregnated onto three different titania supports and was observed W species with very low intensity peaks at 22° and 33°. The 10W/TiO_2-A, 10W/TiO_2-R, and 10W/TiO_2-P25 catalysts show the similar XRD patterns as seen on those for the titania supports and also exhibit weaker intensity than that of the corresponding pure supports.

4.1.3 Scanning electron microscope (SEM) and energy dispersive X-ray spectroscopy (EDX)

The morphologies and element distributions of titania supports having different phases were determined by using scanning electron microscope (SEM) and energy dispersive X-ray spectroscopy (EDX), respectively.

From SEM micrpgraphs in **Figure 9**, TiO_2 supports mostly exhibited irregular shape of particles. In addition, the particles of 10W/TiO_2-R catalyst were smaller than those of 10W/TiO_2-A and 10W/TiO_2-P25 catalysts (in form of catalyst patches).

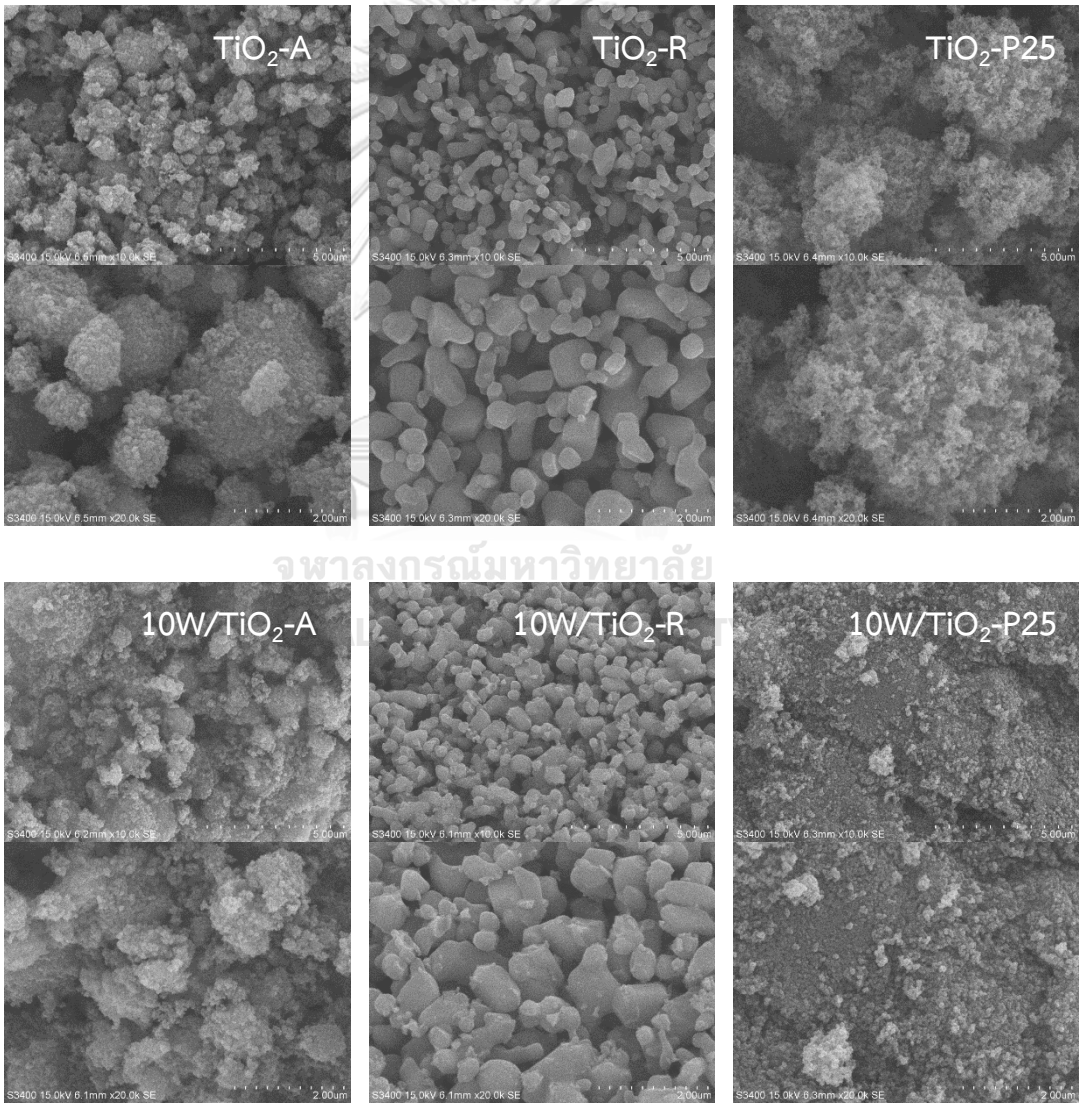

Figure 9 SEM micrographs of supports and catalysts with different phase of TiO_2

The element dispersion of TiO_2 supports and 10W/TiO_2 catalysts with different phase of TiO_2, which were studied through energy dispersive X-ray spectroscopy (EDX), is shown in elemental distribution mapping (EDX mapping) of each catalyst. The EDX mapping of each sample is demonstrated in **Figures 10** to **16** as follows;

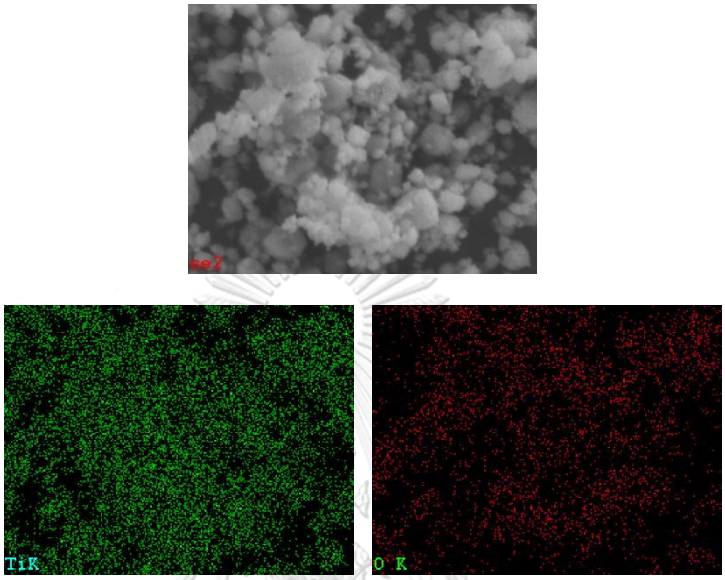

Figure 10 EDX mapping of TiO_2-A

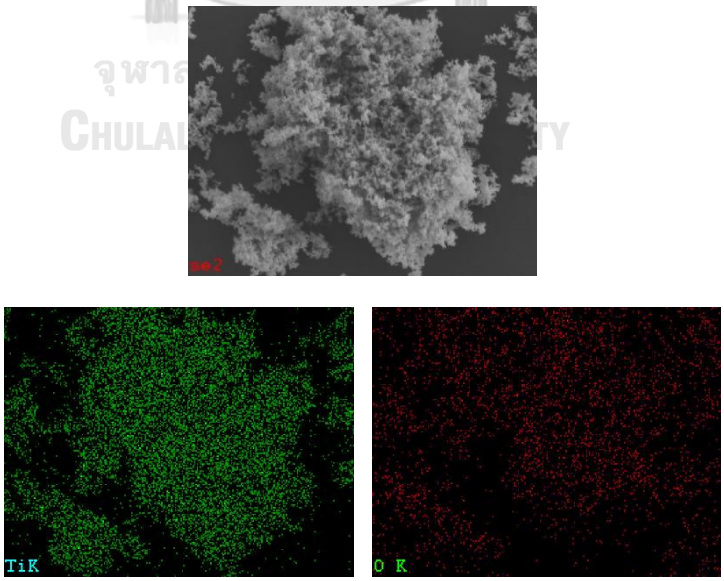

Figure 11 EDX mapping of TiO_2-R

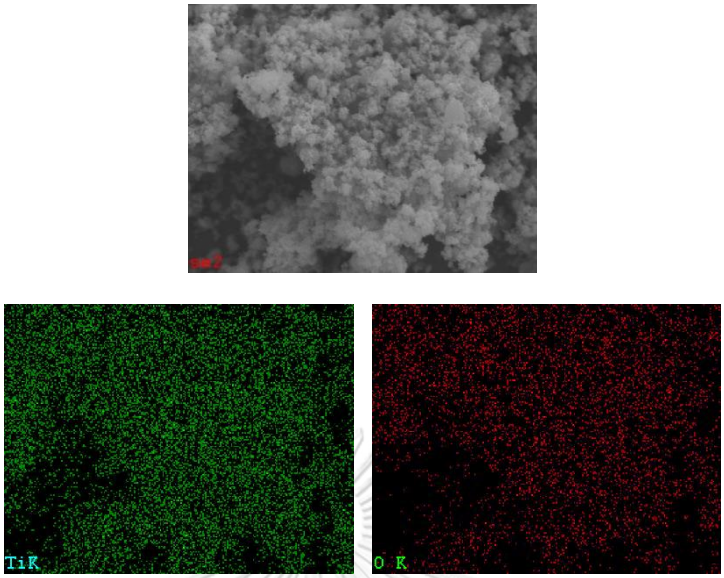

Figure 12 EDX mapping of TiO_2-P25

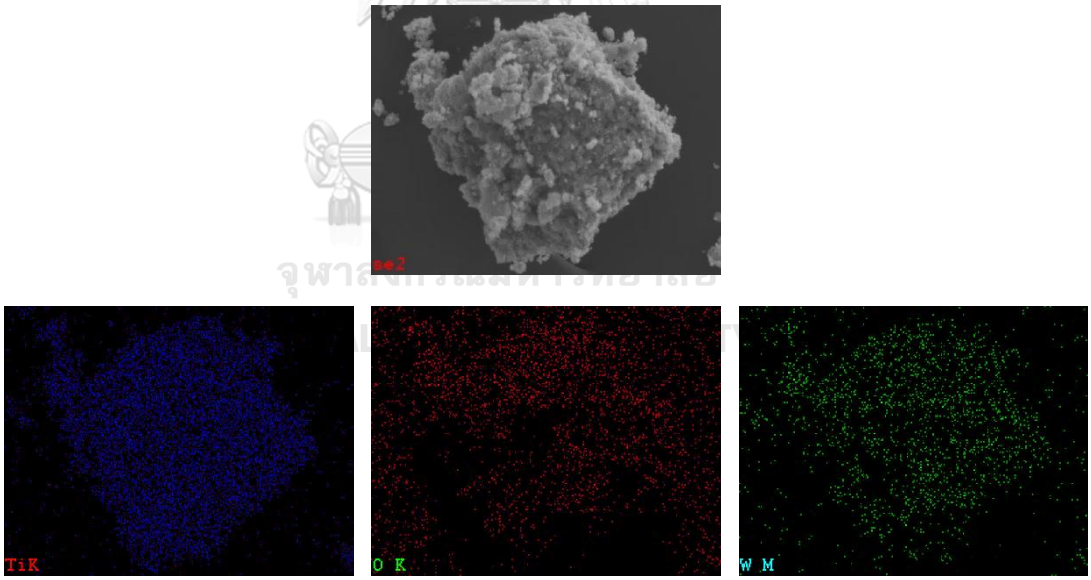

Figure 13 EDX mapping of 10W/TiO_2-A

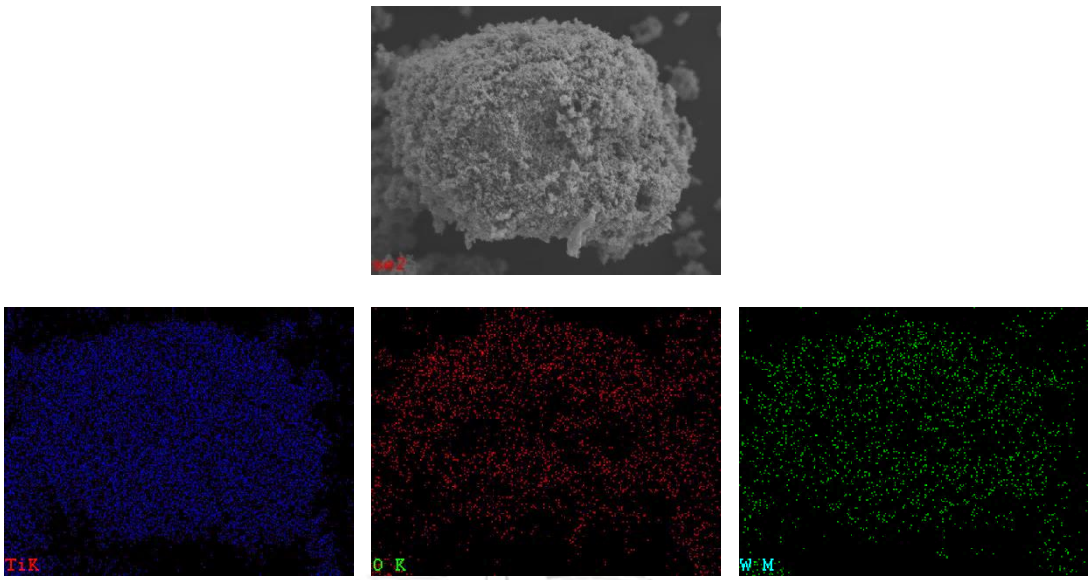

Figure 14 EDX mapping of 10W/TiO_2-R

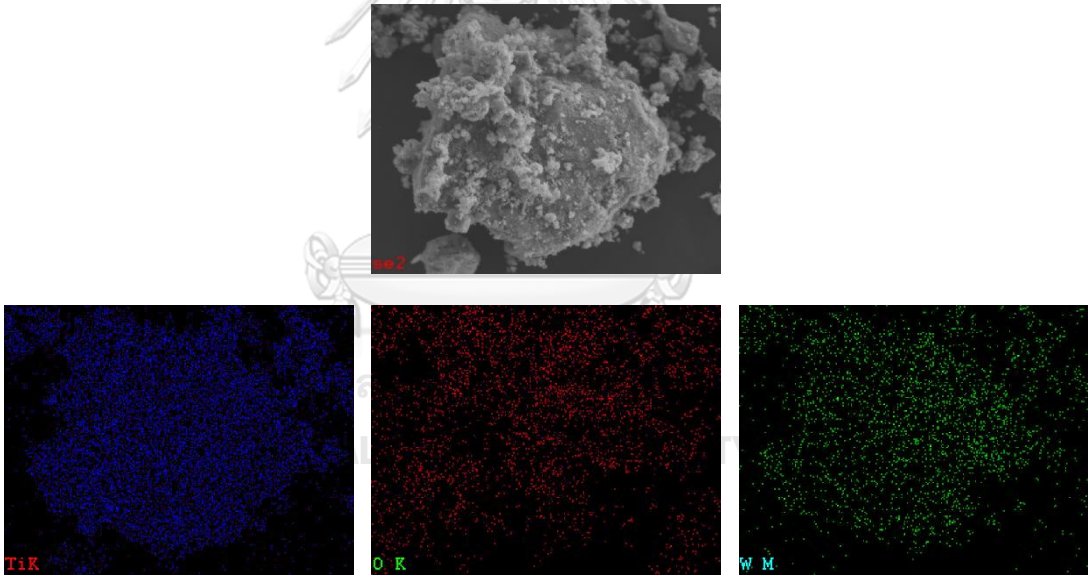

Figure 15 EDX mapping of 10W/TiO_2-P25

From the EDX mappings as seen above, it was found that titanium (Ti), oxygen (O) and tungsten (W) distribution on the surface of catalysts confirms the good distribution of W species on the external surface of catalysts. In addition, the amounts of elemental distribution (Ti, O and W) in weight percent and atom percent on the catalysts surface are displayed in **Table 3**.

Table 3 The amount of elemental distribution on the catalysts surface

Catalysts	Amount of element on surface (wt%)			Amount of element on surface (at%)		
	Ti	O	W	Ti	O	W
TiO_2-A	70.59	29.41	-	44.50	55.50	-
TiO_2-R	69.34	30.66	-	43.03	56.97	-
TiO_2-P25	70.32	29.68	-	44.17	55.83	-
10W/TiO_2-A	58.74	26.37	14.88	41.49	55.77	2.74
10W/TiO_2-R	61.56	26.39	12.05	42.84	54.98	2.19
10W/TiO_2-P25	55.57	29.19	15.25	37.82	59.47	2.70

According to the results from ICP and EDX, it can be proposed that tungsten species had larger particle size than pore size of titania supports. The tungsten species were discovered on the external surface more than the internal pore of catalysts. The amount of tungsten comparing between surface and bulk of catalysts are shown in **Table 4**.

Table 4 The amount of tungsten comparing between surface and bulk of catalysts

Catalysts	Amount of tungsten on surface catalysts identified by EDX (wt%)	Amount of tungsten on bulk catalysts identified by ICP (wt%)
10W/TiO_2-A	14.88	10.66
10W/TiO_2-R	12.05	10.11
10W/TiO_2-P25	15.25	10.22

4.1.4 N_2 physisorption

The texture properties, such as BET surface area, pore volume and pore diameter of TiO_2 supports and 10W/TiO_2 catalysts with different phase of TiO_2 determined by N_2 physisorption are reported in **Table 5**.

Table 5 Textural properties of all supports and catalysts with different phase of TiO_2

Catalysts	BET surface area (m^2/g)	Pore volume (cm^3/g)	Pore diameter (nm)
TiO_2-A	58	0.24	11.9
TiO_2-R	7	0.01	10.7
TiO_2-P25	47	0.13	9.3
10W/TiO_2-A	51	0.29	19.3
10W/TiO_2-R	8	0.01	8.1
10W/TiO_2-P25	53	0.30	18.9

The surface area analyzed by BET method, pore volume and pore diameter analyzed by BJH method show that TiO_2-A had a significantly higher surface area (58 m^2/g) and pore volume (0.24 cm^3/g) relative to TiO_2-R surface area (7 m^2/g) and pore volume (0.01 cm^3/g). Besides two pure phase supports, TiO_2-P25 containing mostly anatase had similar surface area (47 m^2/g) and pore volume (0.13 cm^3/g) to TiO_2-A. Moreover, 10W/TiO_2-A and 10W/TiO_2-P25 catalysts also exhibited higher surface areas and pore volume than that of W/TiO_2-R catalyst. Therefore, the addition of tungsten onto titania supports slightly changed the textural properties.

Moreover, the N_2 adsorption-desorption isotherms at -196°C for the catalysts with different phase of TiO_2 are illustrated in **Figure 16**. It was found that all supports and catalysts presented type IV isotherms with the type H1 hysteresis loops at high relative pressure ($0.7<P/P_0<0.9$) according to the IUPAC classification, which confirm the mesopososity of the catalysts. It can be seen that the hysteresis loop for both anatase and P25 supports are broader indicating larger pore volume than rutile support. This result can be further confirmed by the corresponding pore volume, as shown in **Table 5**. It can be found that TiO_2-A had larger pore volume (0.24 cm^3/g) than that of other supports. Furthermore, the addition of tungsten onto titania supports can be slightly increased pore volume.

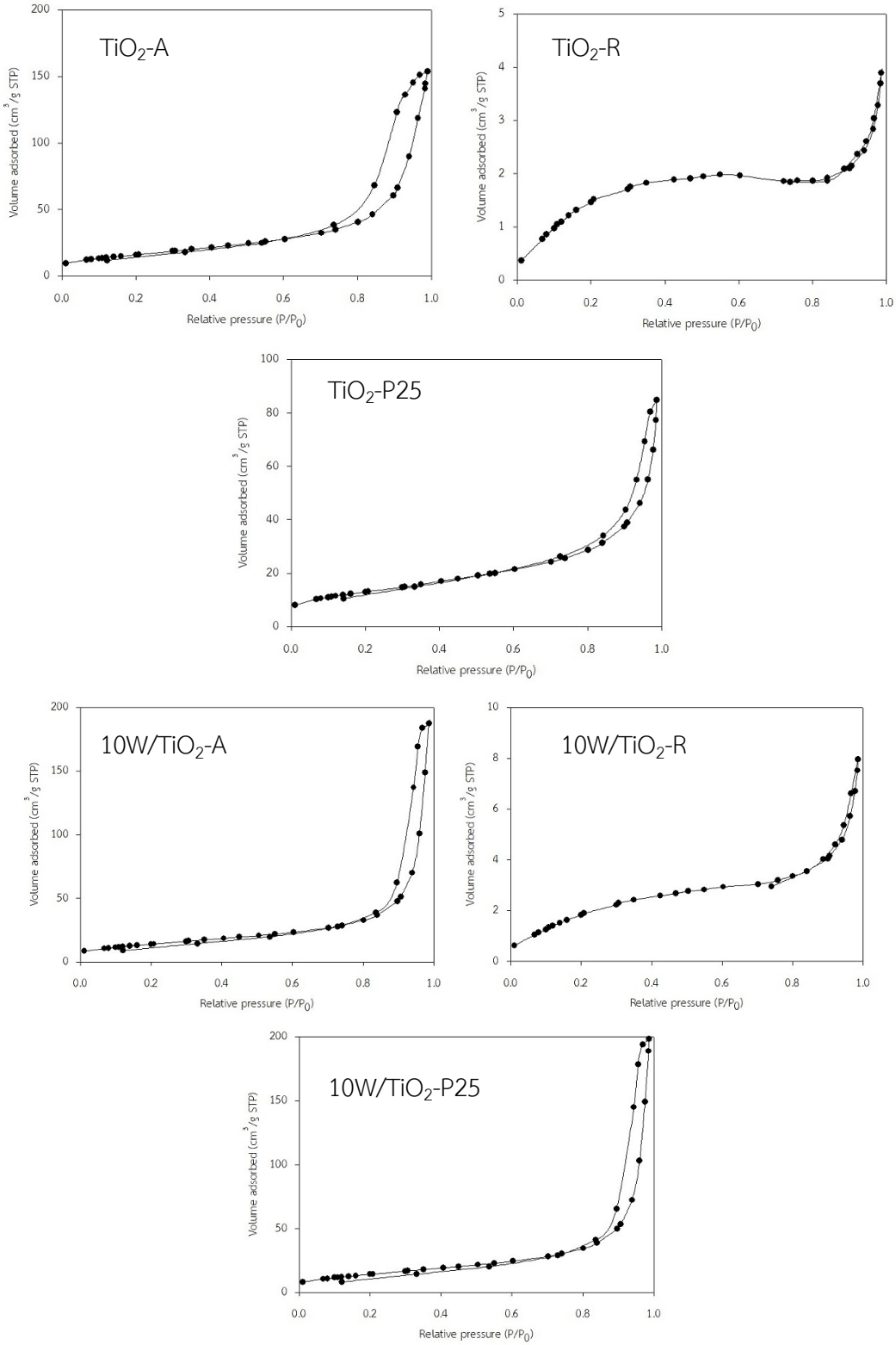

Figure 16 The N_2 adsorption-desorption isotherms of all supports and catalysts with different phase of TiO_2

4.1.5 Ammonia temperature-programmed desorption (NH_3-TPD)

The acidity of all supports and catalysts were characterized by using ammonia temperature-programmed desorption (NH_3-TPD) and shown in **Figure 17**. The NH_3-TPD profiles of TiO_2-A, TiO_2-P25, 10W/TiO_2-A and 10W/TiO_2-P25 samples were found to have broad desorption peaks in range between 150 and 500°C, whereas TiO_2-R and 10W/TiO_2-R can not be found any desorption peaks. Normally, the desorption peaks at low temperature (below 250°C) represent weak acid sites, whereas those at temperature above 250°C correspond to medium-strong acid sites. The area under broad peaks were calculated in order to show the acidity of samples.

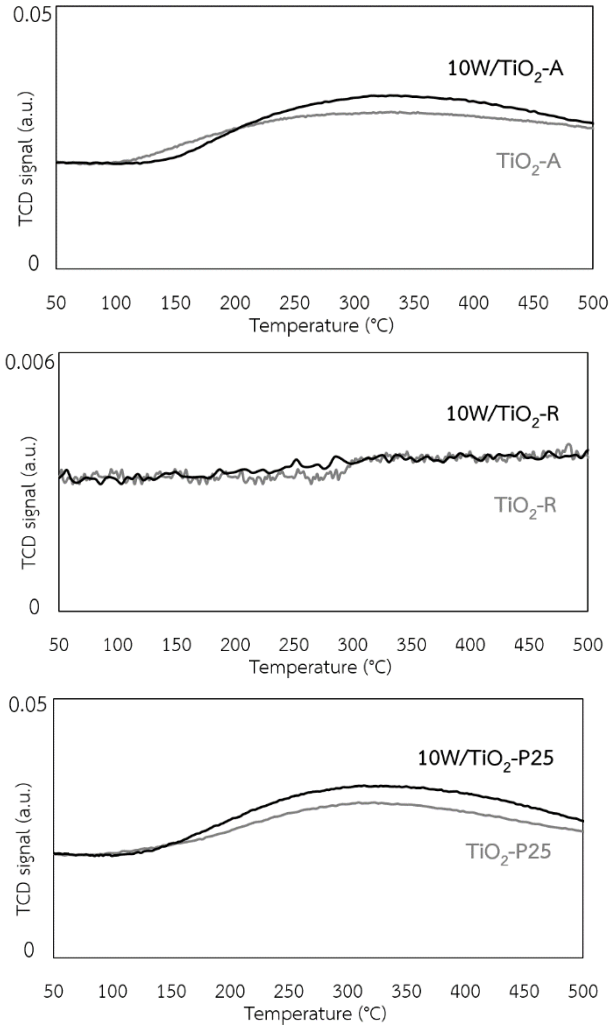

Figure 17 NH_3-TPD profiles of TiO_2 supports and 10W/TiO_2 catalysts with different phases of TiO_2

The total acidic property of all supports and catalysts is reported in **Table 6**. TiO_2 supports (anatase, rutile and P25) present total acid site of 1639, 75 and 1866 μmol/g cat, respectively. After impregenated 10 wt% W into all supports, catalysts increased areas under TCD signal curve relating to the amount of acid sites. It was found that 10W/TiO_2-P25 catalyst had the highest amount of total acid sites of 2247 μmol/g cat.

Table 6 The amount of acidity of supports and catalysts with different phase of TiO_2

catalysts	**Total acidity (μmol/g cat.)**
TiO_2-A	1639
TiO_2-R	75
TiO_2-P25	1866
10W/TiO_2-A	2137
10W/TiO_2-R	112
10W/TiO_2-P25	2247

4.1.6 Reaction test

To measure the catalytic properties for TiO_2 supports and 10W/TiO_2 catalysts having different phase of titania, the catalytic ethanol dehydration was performed at the reaction temperature range of 200 to 400°C. The result of ethanol conversions is shown in **Figure 18**. It was found that ethanol conversion obviously increased with increasing the reaction temperatures for all supports and catalysts indicating no deactivation of catalysts upto 400°C. The 10W/TiO_2-P25 catalyst exhibited the highest ethanol conversion (66.2%) among other catalysts for all reaction temperatures.

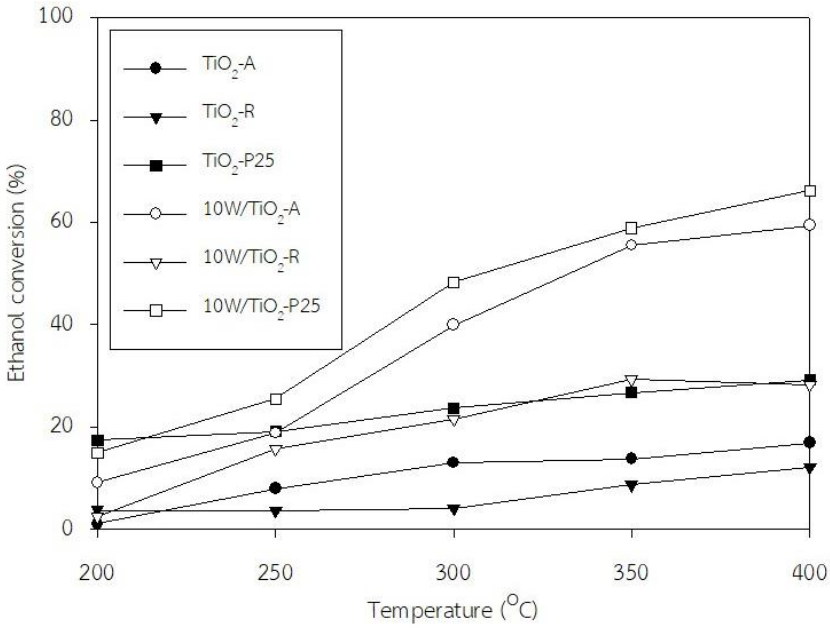

Figure 18 Ethanol conversion of TiO_2 supports and 10W/TiO_2 catalysts with different phase of TiO_2

The product selectivities obtained from all supports and catalysts are shown in **Figure 19**. For pure TiO_2 supports, acetaldehyde was mainly produced in all reaction temperatures and then ethylene was formed with increasing the reaction temperature, as shown in **Figure 19 (a)**. Moreover, it is known that ethylene is obtained via endothermic reaction. It can be observed that ethylene selectivity increased with increasing reaction temperatures. From the results illustrate in **Figure 19 (b)**, 10W/TiO_2-P25 catalyst produced slightly higher ethylene selectivity than other catalysts. However, the formation of diethyl ether is favored by exothermic reaction, thus, increasing the reaction temperatures apparently resulted in decreasing diethyl ether selectivity based on the fact that diethyl ether is decomposed to ethylene at the high temperature. At the low temperature (below 300°C), 10W/TiO_2-A and 10W/TiO_2-P25 catalysts produced higher diethyl ether selectivity than 10W/TiO_2-R catalyst. Especially at 200°C, W/TiO_2-R catalyst can not produce any diethyl ether. Besides two products, acetaldehyde was well formed as a byproduct for 10W/TiO_2-R catalyst.

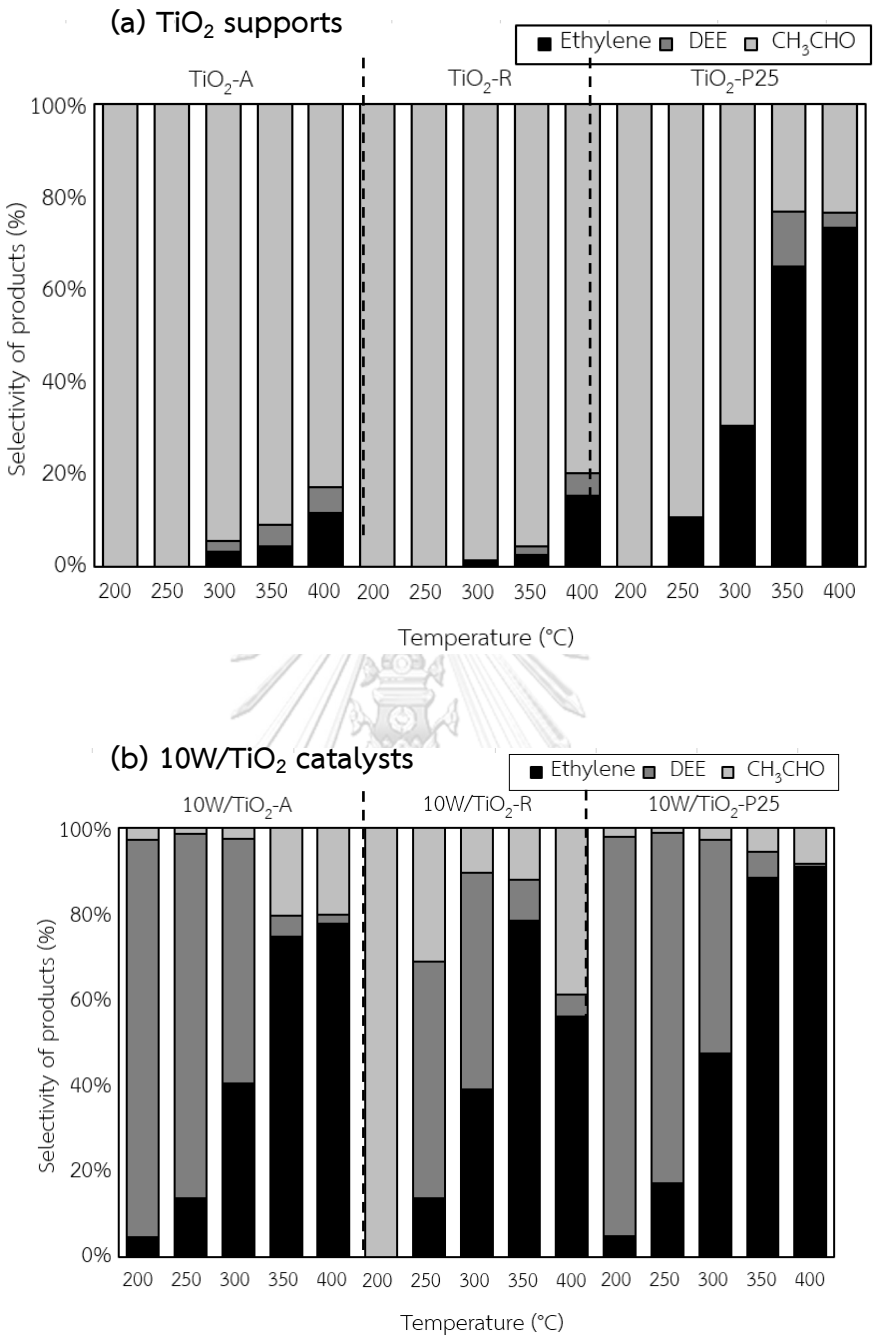

Figure 19 Product selectivities of **(a)** TiO_2 supports and **(b)** 10W/TiO_2 catalysts with different phase of TiO_2

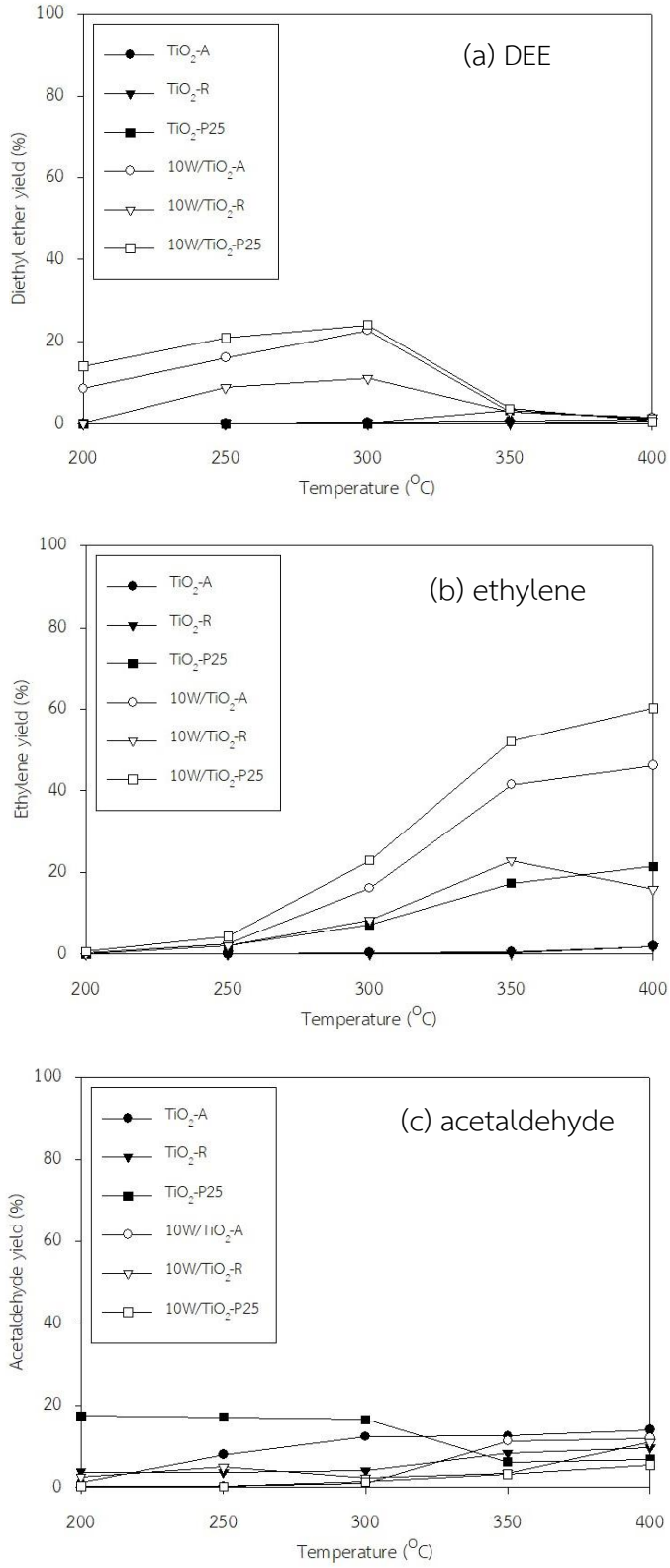

Figure 20 Product yields of TiO_2 supports and 10W/TiO_2 catalysts with different phase of TiO_2

A comparison of product yields of all supports and catalysts is shown in **Figure 20**. The yield of each product is defined as ethanol conversion multiply with their selectivity.

From **Figure 20 (a)** above, it shows the DEE yield of TiO_2 supports and 10W/TiO_2 catalysts with different phase of TiO_2. The results showed that all TiO_2 supports having tungsten can produce higher DEE yield than pure TiO_2 supports. All W/TiO_2 catalyst yields increased with increasing the reaction temperature up to 300°C. In addition, at 300°C, 10W/TiO_2-P25 catalyst gave the highest DEE yield (24.1%) among all catalysts and reaction temperatures. After further increasing the reaction temperature, DEE yield decreased due to the lower DEE selectivity.

In **Figure 20 (b)**, the trend of ethylene yield is reported. Ethylene yield was increased with increasing the reaction temperature because ethanol conversion and ethylene selectivity also increased as seen in **Figure 18** and **Figure 19**. Moreover, the highest ethylene yield of 60.3% was obtained from 10W/TiO_2-P25 catalysts at 400°C. Besides two products, acetaldehyde was formed as a byproduct for TiO_2 supports without tungsten deposition as resulted in **Figure 20 (c)**.

Based on these results as reported in **Table 7**, it can be summarized that the phase composition of titania support can affect the catalytic behavior of W/TiO_2 catalysts. The mixed phases of anatase and rutile titania is more suitable for W probably due to higher surface properties of catalyst. They were the factors leading to get higher activity for ethanol dehydration of the catalyst on mixed phase (P25) than other phases. Therefore, TiO_2-P25 support was selected to further study the effect of tungsten loading on ethanol dehydration reaction.

Table 7 Ethanol conversion, product selectivities and product yields

Catalyst	Temperature (°C)	Ethanol Conversion (%)	Product Selectivity (%)			Product Yield (%)		
			Ethylene	DEE	CH_3CHO	Ethylene	DEE	CH_3CHO
TiO_2-A	200	1.15	0.0	0.0	100.0	0.0	0.0	1.2
	250	7.99	0.0	0.0	100.0	0.0	0.0	8.0
	300	13.05	3.2	2.2	94.6	0.4	0.3	12.3
	350	13.77	4.5	4.6	90.9	0.6	0.6	12.5
	400	16.93	11.6	5.7	82.7	2.0	1.0	14.0
TiO_2-R	200	3.78	0.0	0.0	100.0	0.0	0.0	3.8
	250	3.70	0.0	0.0	100.0	0.0	0.0	3.7
	300	4.11	1.4	0.0	98.6	0.1	0.0	4.1
	350	8.75	2.5	1.9	95.6	0.2	0.2	8.4
	400	12.21	15.4	4.8	79.9	1.9	0.6	9.8
TiO_2-P25	200	17.44	0.0	0.0	100.0	0.0	0.0	17.4
	250	19.19	10.6	0.0	89.4	2.0	0.0	17.2
	300	23.72	30.3	0.0	69.7	7.2	0.0	16.5
	350	26.78	65.0	11.8	23.2	17.4	3.2	6.2
	400	29.26	73.3	3.3	23.4	21.5	1.0	6.8
10W/TiO_2-A	200	9.2	4.5	92.7	2.8	0.4	8.5	0.3
	250	18.8	13.8	84.9	1.4	2.6	16.0	0.3
	300	39.9	40.5	57.0	2.5	16.2	22.8	1.0
	350	55.6	74.7	4.9	20.3	41.5	2.7	11.3
	400	59.5	77.7	2.2	20.1	46.2	1.3	12.0
10W/TiO_2-R	200	2.4	0.0	0.0	100.0	0.0	0.0	2.4
	250	15.7	13.6	55.3	31.1	2.1	8.7	4.9
	300	21.5	39.0	50.7	10.3	8.4	10.9	2.2
	350	29.3	78.5	9.5	12.0	23.0	2.8	3.5
	400	28.3	56.1	5.2	38.7	15.9	1.5	11.0
10W/TiO_2-P25	200	15.0	4.7	93.4	1.9	0.7	14.0	0.3
	250	25.5	17.1	81.8	1.1	4.4	20.9	0.3
	300	48.3	47.4	49.8	2.7	22.9	24.1	1.3
	350	58.9	88.5	6.1	5.4	52.1	3.6	3.2
	400	66.2	91.1	0.7	8.2	60.3	0.4	5.4

4.1.7 Thermal gravimetric analysis (TGA)

To determine the coke formation, the spent catalysts were analyzed by using thermal gravimetric analysis (TGA) as shown in **Figure 21**. It can be seen that TGA curves of all spent catalysts using in the reaction exhibited similar activity. At temperature below 200°C, the weight of catalyst is lost due to the water elimination. At high temperature (200-1000°C), the weight loss may be the burning of coke on the surface of spent catalyst.

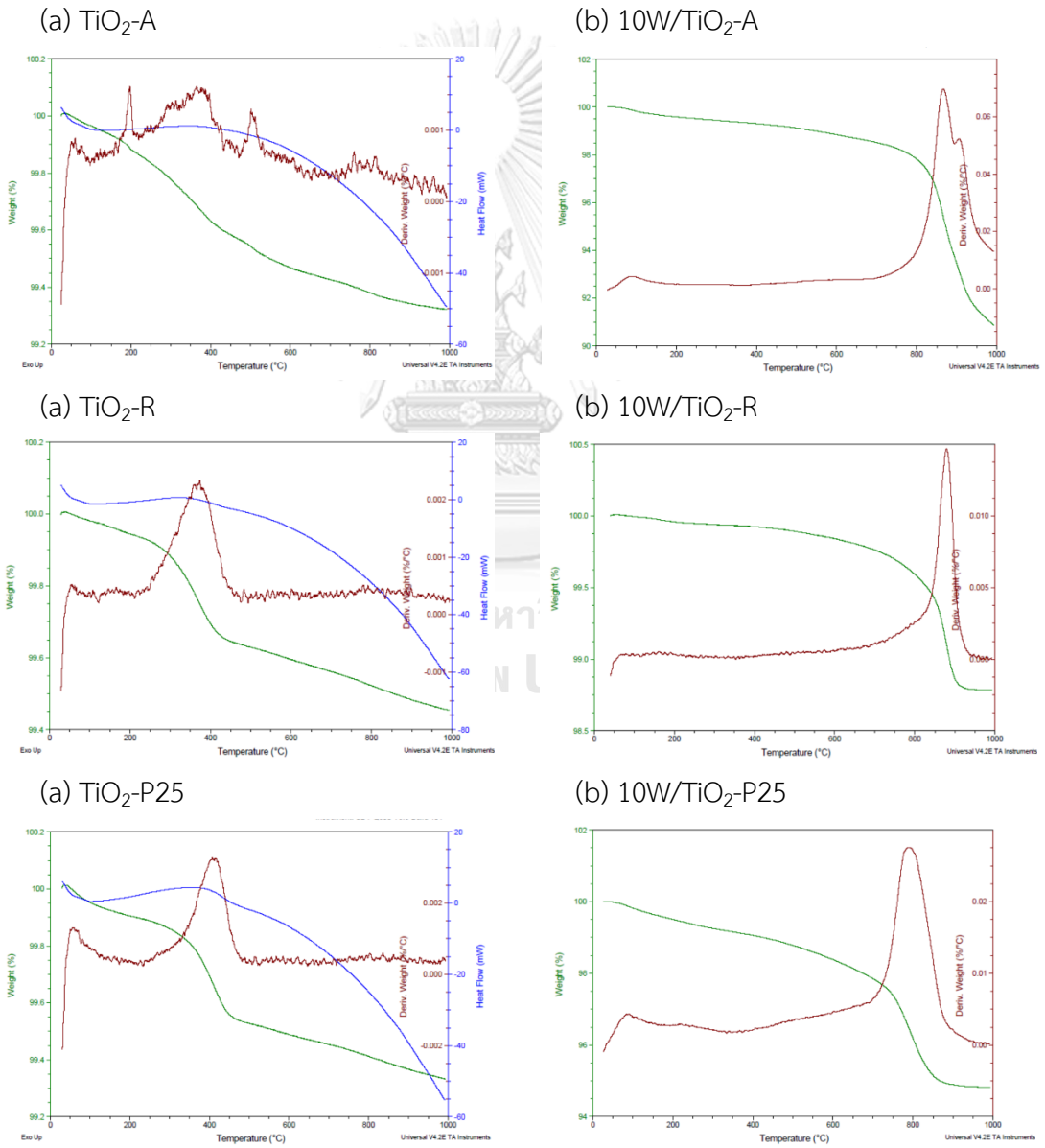

Figure 21 TGA analysis curves of spent catalysts

At temperature higher that 200°C, it was found that 10W/TiO_2 catalysts displayed higher weight loss than pure TiO_2 supports. This is because the interaction between W and TiO_2 support introducing the catalyst burning. The amount of coke formation in spent catalysts was determined and reported in **Table 8**.

Table 8 The amount of coke formation in the spent catalysts

Catalyst	Temperature (°C)	Weight (%)	The amount of coke formation (%)
TiO_2-A	200	99.88	0.56
	1000	99.32	
TiO_2-R	200	99.94	0.49
	1000	99.45	
TiO_2-P25	200	99.91	0.58
	1000	99.33	
10W/TiO_2-A	200	99.59	8.74
	1000	90.89	
10W/TiO_2-R	200	99.96	1.18
	1000	98.78	
10W/TiO_2-P25	200	99.51	4.71
	1000	94.82	

4.1.8 Catalyst appearance

Three different TiO_2 (anatase, rutile and P25) supports were brought to observe the appearance before and after being used in ethanol dehydration reaction. The appearance of fresh and spent supports and catalysts with different phases of TiO_2 is presented in **Figures 22** and **23**, respectively.

Figure 22 The appearance of fresh supports and catalysts
(a) TiO_2-A (b) TiO_2-R (c) TiO_2-P25 (d) 10W/TiO_2-A (e) 10W/TiO_2-R (f) 10W/TiO_2-P25

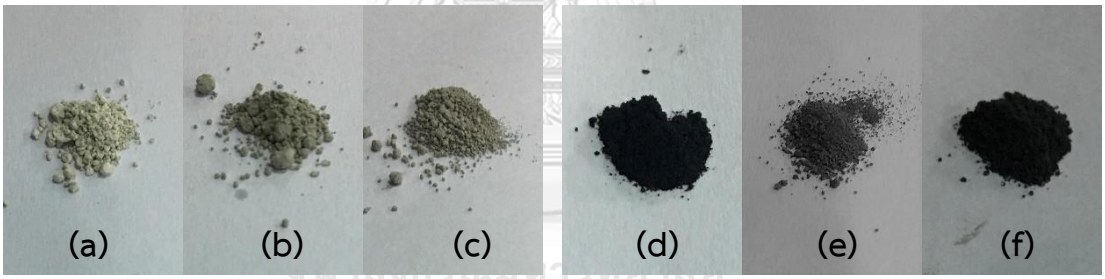

Figure 23 The appearance of spent supports and catalysts
(a) TiO_2-A (b) TiO_2-R (c) TiO_2-P25 (d) 10W/TiO_2-A (e) 10W/TiO_2-R (f) 10W/TiO_2-P25

The appearances of fresh TiO_2 supports are white, whereas 10W/TiO_2 catalysts are yellow due to the presence of tungsten in surface of catalyst. After all samples were performed in ethanol dehydration reaction, the spent catalysts were observed that the presence of tunsten in catalyst caused higher the coke formation than pure TiO_2 supports as confirmed in TGA analysis.

Part II : The characteristic and catalytic activity of W/TiO_2-P25 catalysts with different loading of tungsten (0-20 wt% W)

After comparing the different phases of TiO_2 support, it was found that 10W/TiO_2-P25 catalyst gave the highest diethyl ether yield of 24.1% at 300°C in ethanol dehydration reaction. Thus, TiO_2-P25 support was then chosen in order to elucidate the effect of W loading in the similar way. This part was also studied both catalytic properties and performance in ethanol dehydration.

4.2.1 Inductively coupled plasma (ICP)

After prepared TiO_2-P25 support with different loading of tungsten pior to the method, the obtained W/TiO_2-P25 catalysts were brought to determine the amount of tungsten in bulk catalyst by inductively coupled plasma (ICP) as shown in **Table 9**.

Table 9 The amount of tungsten contained in bulk catalysts

Catalysts	Amount of W in bulk catalysts (wt%)
5W/TiO_2-P25	4.87
10W/TiO_2-P25	10.22*
15W/TiO_2-P25	15.61
20W/TiO_2-P25	20.45

* taken from **Part I**

From ICP result, the obtained catalysts were called 5W/TiO_2-P25, 10W/TiO_2-P25, 15W/TiO_2-P25 and 20W/TiO_2-P25 for the contents of 5, 10, 15 and 20 wt% of tungsten, respectively.

4.2.2 X-ray diffraction (XRD)

XRD patterns of TiO_2-P25 support and W-modified TiO_2-P25 catalysts containing the different loading of 5, 10, 15 and 20 wt% W are presented in **Figure 24**. XRD peaks of W/TiO_2-P25 catalysts was similar as already explained in **Part I**. No peak of tungsten cannot be detected up to 10 wt% by XRD, indicating a good dispersion of tungsten on the surface of TiO_2-P25 support. However, above 10 wt% W, the crystalline phase of tungsten from the decomposition of ammonium metatungstate was observed.

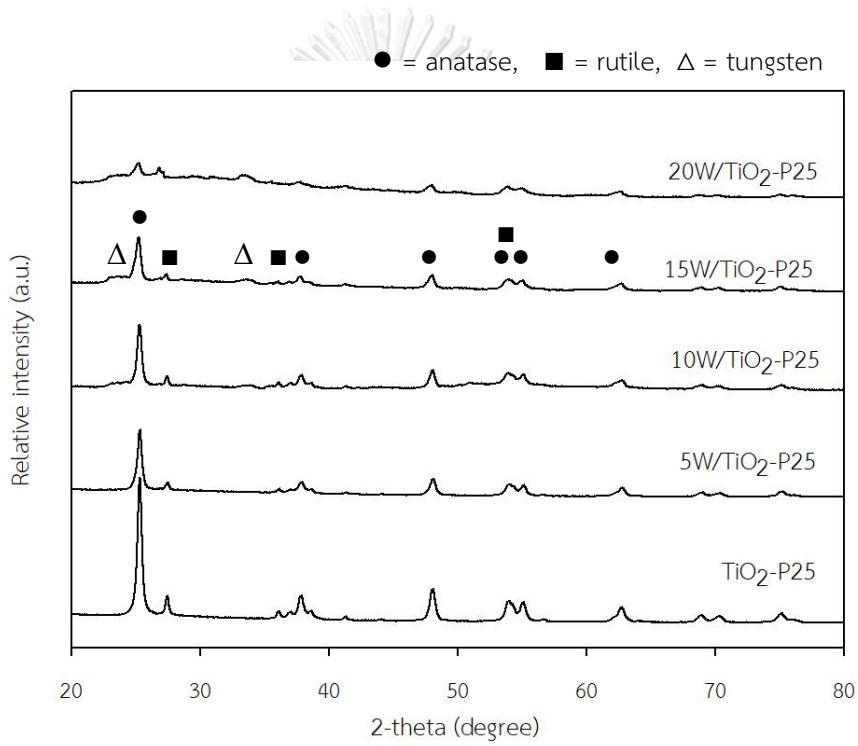

Figure 24 XRD patterns of TiO_2-P25 support and W/TiO_2-P25 catalysts

4.2.3 Scanning electron microscope (SEM) and energy dispersive X-ray spectroscopy (EDX)

The morphology and elemental distribution of W/TiO_2-P25 catalysts having different loading contents of tungsten (0-20 wt%) were observed by using scanning electron microscope (SEM) as shown in **Figure 25** and energy dispersive X-ray spectroscopy (EDX) as shown in **Figures 26** to **30**, respectively.

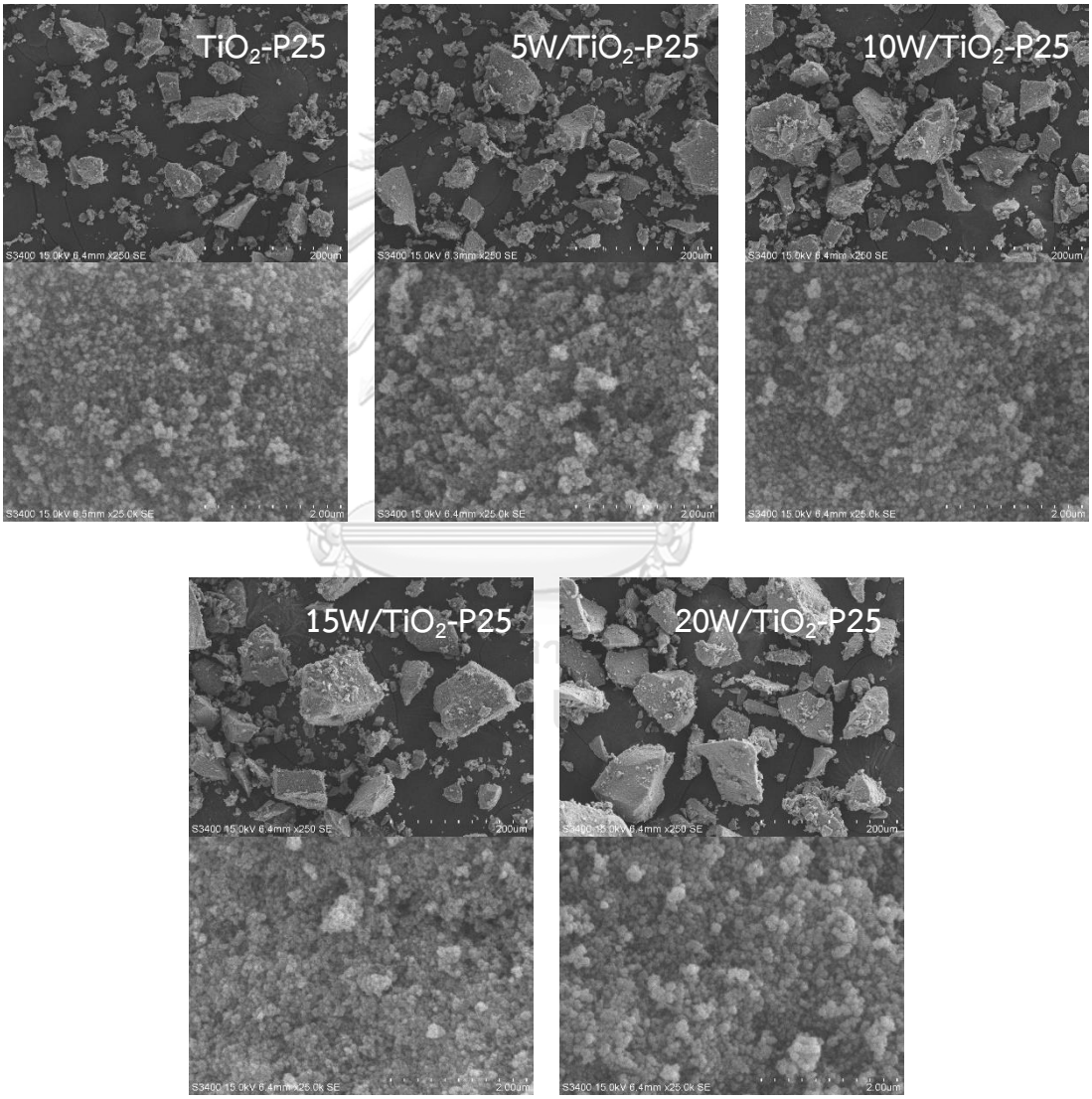

Figure 25 SEM micrographs of TiO_2-P25 support and W/TiO_2-P25 catalysts

SEM micrpgraphs of TiO_2-P25 support and W/TiO_2-P25 catalysts having different loading contents of tungsten (0-20 wt%) in **Figure 25** reveal that all of the obtained catalysts had irregular shape of particles. Moreover, the amount of tungsten loading into the catalysts did not change the catalyst morphologies indicating the similar morphological structures.

The element dispersion of TiO_2-P25 support and W/TiO_2-P25 catalysts having different loading contents of tungsten (0-20 wt%) are displayed in EDX mapping and demonstrated in **Figures 26** to **30** as follows;

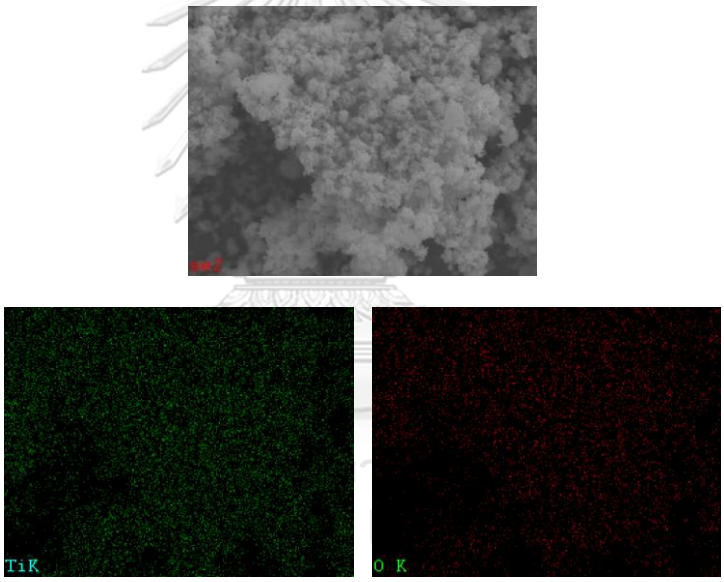

Figure 26 EDX mapping of TiO_2-P25

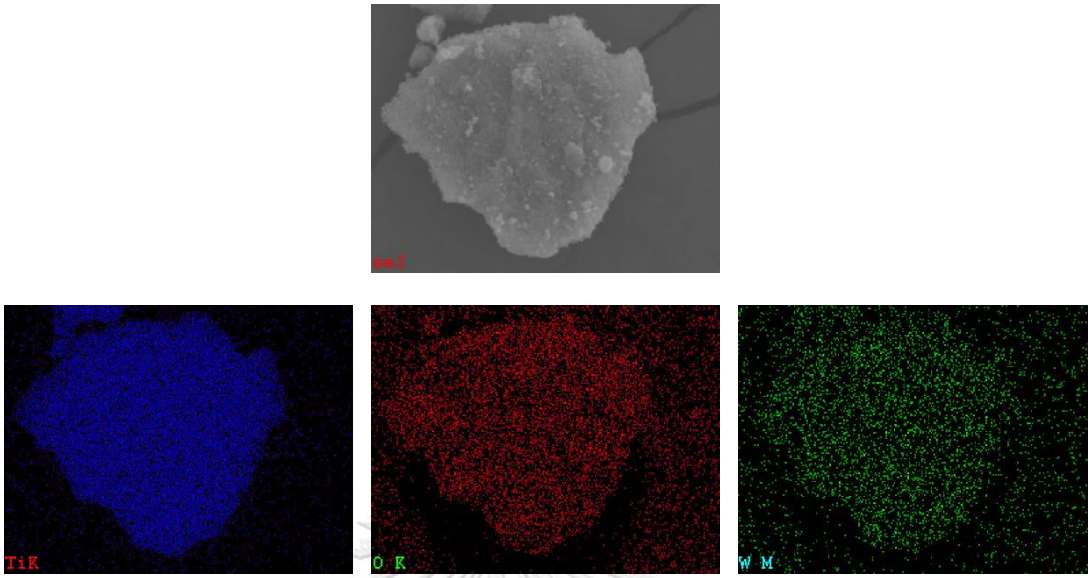

Figure 27 EDX mapping of 5W/TiO_2-P25

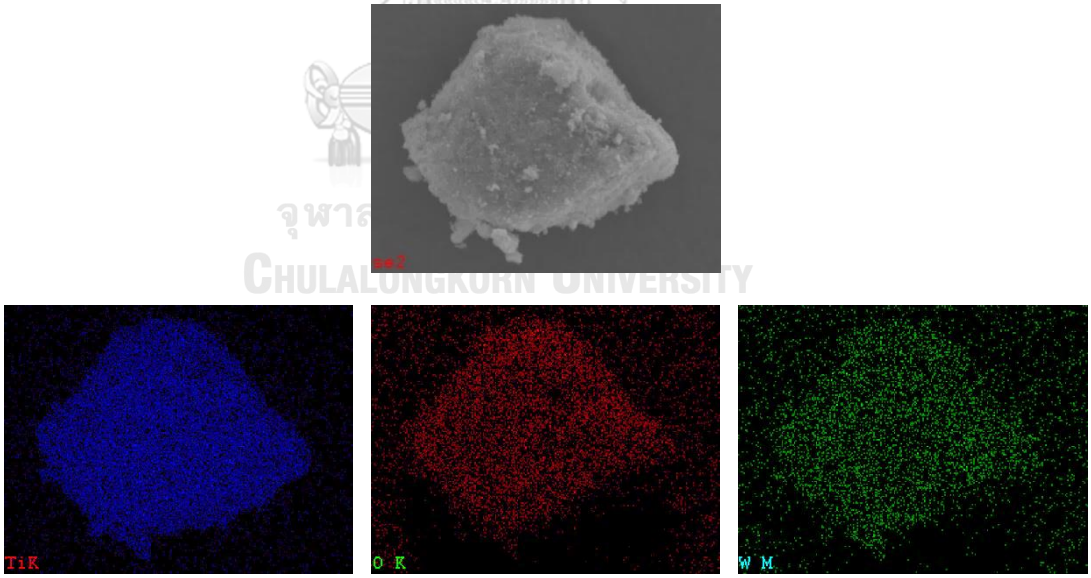

Figure 28 EDX mapping of 10W/TiO_2-P25

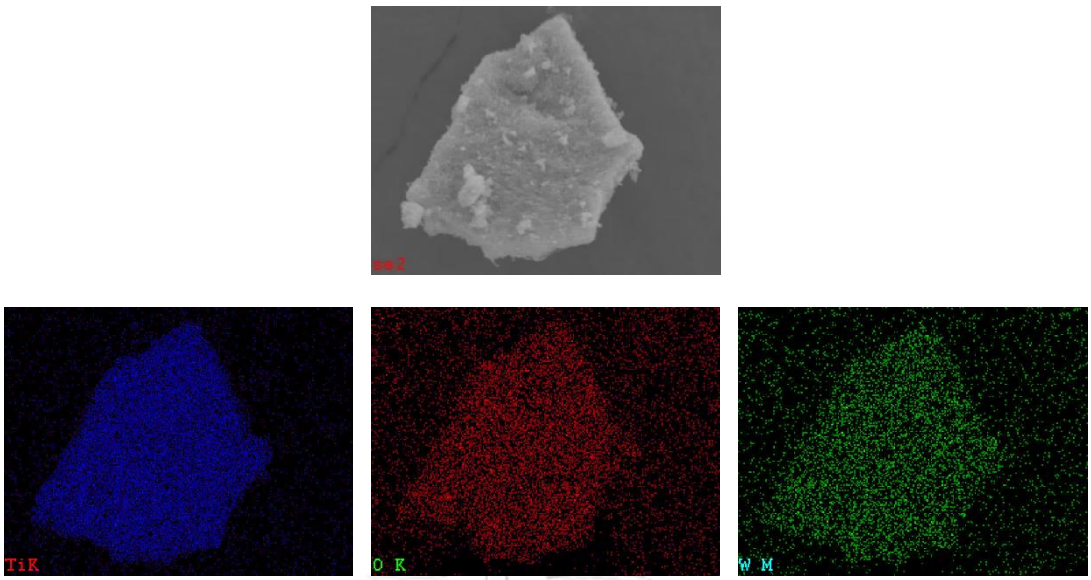

Figure 29 EDX mapping of 15W/TiO_2-P25

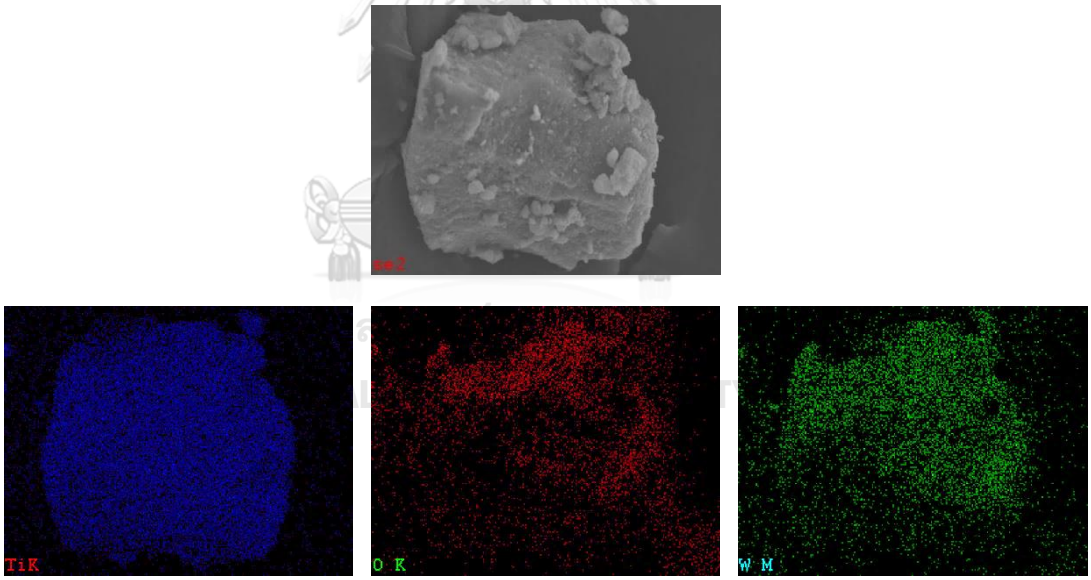

Figure 30 EDX mapping of 20W/TiO_2-P25

From the EDX mappings shown above, the elemental composition of W/TiO_2-P25 catalyst consisting Ti, O and W can be seen by the different colour dots, which confirms the good distribution of W on the external surface of W/TiO_2-P25 catalysts.

Moreover, the quantity of elemental distribution (Ti, O and W) in weight percent and atom percent on the catalysts surface can also be measured by EDX and are summarized in **Table 10**

Table 10 The amount of elemental distribution on the catalysts surface

Catalysts	Amount of element on surface (wt%)			Amount of element on surface (at%)		
	Ti	O	W	Ti	O	W
TiO_2-P25	70.32	29.68	-	44.17	55.83	-
5W/TiO_2-P25	53.96	41.42	4.63	30.12	69.21	0.67
10W/TiO_2-P25	55.57	29.19	15.25	37.82	59.47	2.70
15W/TiO_2-P25	59.47	24.05	16.48	43.80	53.04	3.16
20W/TiO_2-P25	55.61	23.44	20.06	42.39	53.45	4.16

From Both of ICP and EDX results, it can be concluded that tungsten species were found on the external surface more than the internal pore of catalysts since tungsten had larger size than the pore of catalyst as similar to **Part I**. The amount of tungsten comparing between surface and bulk of catalysts are shown in **Table 11** as follows;

Table 11 The amount of tungsten comparing between surface and bulk of catalysts

Catalysts	Amount of tungsten on surface catalysts identified by EDX (wt%)	Amount of tungsten on bulk catalysts identified by ICP (wt%)
5W/TiO_2-P25	4.63	4.87
10W/TiO_2-P25	15.25	10.22
15W/TiO_2-P25	16.48	15.61
20W/TiO_2-P25	20.06	20.45

4.2.4 N_2 physisorption

The BET surface area, pore volume and pore diameter of catalysts with different loading of tungsten determined by N_2 physisorption are summarized in **Table 12**.

Table 12 Textural properties of W/TiO_2 catalysts with different loading of W

Catalysts	BET surface area (m^2/g)	Pore volume (cm^3/g)	Pore diameter (nm)
TiO_2-P25	47	0.13	9.3
5W/TiO_2-P25	51	0.36	21.5
10W/TiO_2-P25	53	0.30	18.9
15W/TiO_2-P25	56	0.29	20.3
20W/TiO_2-P25	46	0.23	20.3

The addition of W slightly influences the BET surface area in comparison with TiO_2-P25 support. BET surface areas of W/TiO_2-P25 catalysts are higher than that of TiO_2-P25 support, showing that surface area increases gradually with increasing W loading up to 15 wt% W. It is likely that the interaction between W and TiO_2-P25 protects catalysts from sintering. Thus, 15W/TiO_2-P25 catalyst had the highest surface area of 56 m^2/g. However, the addition of W onto TiO_2-P25 can be slightly decreased pore volume, due to W blocked on support pores. Moreover, pore diameter of W/TiO_2-P25 catalysts did not significantly change with the presence of tungsten.

In addition, the N_2 physisorption isotherms of W/TiO_2-P25 catalysts with different W loading (0-20 %wt) are shown in **Figure 31**. All catalysts display type IV isotherms with the type H1 hysteresis loops indicating the mesoporous-typical catalyst.

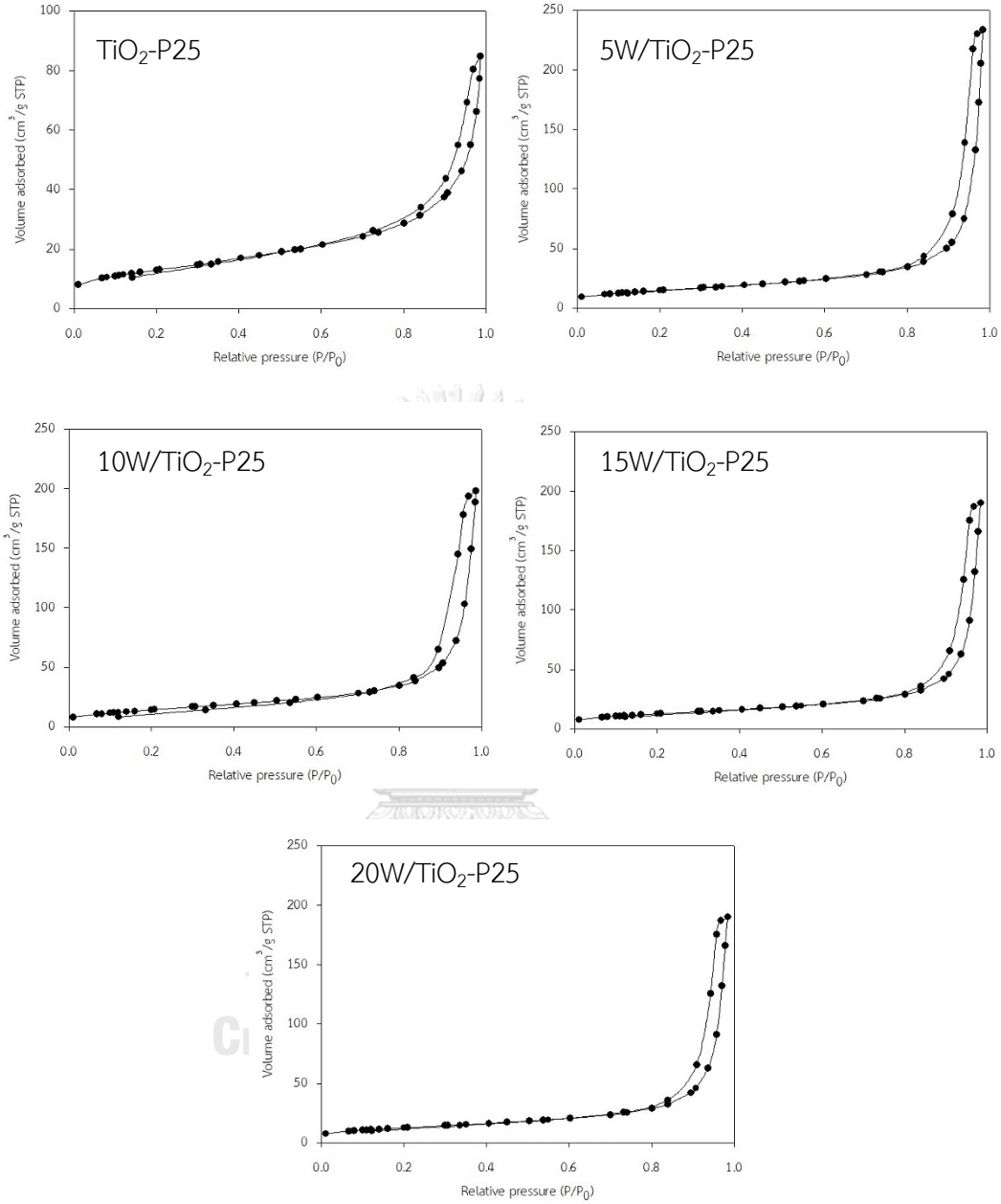

Figure 31 The N_2 adsorption-desorption isotherms of W/TiO_2-P25 catalysts with different loading of W

4.2.5 Ammonia temperature-programmed desorption (NH_3-TPD)

The acid strength of all obtained catalysts was analyzed by using NH_3-TPD. The NH_3-TPD profiles of all samples were found to have similar broad desorption peaks as shown in **Figure 32**.

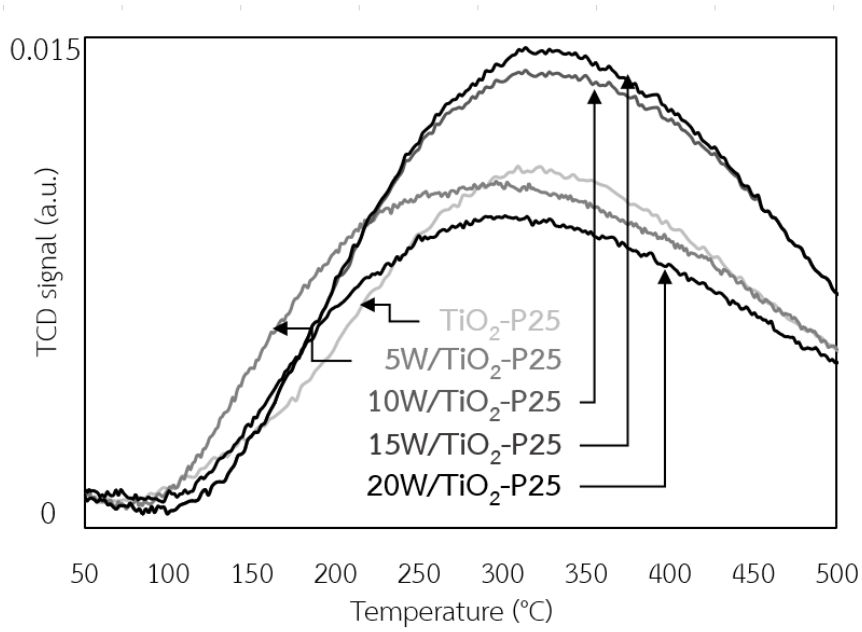

Figure 32 NH_3-TPD profiles of TiO_2-P25 support and W/TiO_2-P25 catalysts with different W loading

The addition of tungsten up to 15 wt% increased area under TCD signal indicating increased acidic property, which was in range of 1820 to 2304 μmol/g cat as demonstrated in **Table 13**. For the addition of tungsten over 15 wt%, the total acidity was decreased demonstrating the deactivated catalyst. Moreover, 15W/TiO_2-P25 catalyst exhibited the highest amount of total acid sites of 2304 μmol/g cat that is excellent characteristic to produce DEE.

Table 13 The amount of acidity of TiO_2-P25 support and W/TiO_2-P25 catalysts with different W loading

catalysts	Total acidity (μmol/g cat.)
TiO_2-P25	1866
5W/TiO_2-P25	1820
10W/TiO_2-P25	2247
15W/TiO_2-P25	2304
20W/TiO_2-P25	1496

4.2.6 Reaction test

Besides the catalytic activity of catalysts having different phases of TiO_2, W/TiO_2-P25 catalysts were investigated with different W loading contents (0-20 wt%) and examined via ethanol dehydration at various reaction temperatures (range of 200 to 400°C). The catalytic activities (ethanol conversion, product selectivities and product yields) of each catalyst is displayed as follows.

The ethanol conversion of these TiO_2-P25 support and W/TiO_2-P25 catalysts is evaluated by ethanol dehydration reaction, and the corresponding results are shown in **Figure 33**. It was found that ethanol conversion apparently increased with increasing the reaction temperature over all catalysts. Considering the different W loading contents, the addition of tungsten over 15 wt% W results to decrease ethanol conversion due to decreased surface area. Thus, 15W/TiO_2-P25 catalyst gave the highest ethanol conversion of 73.94% among all catalysts for all reaction temperature.

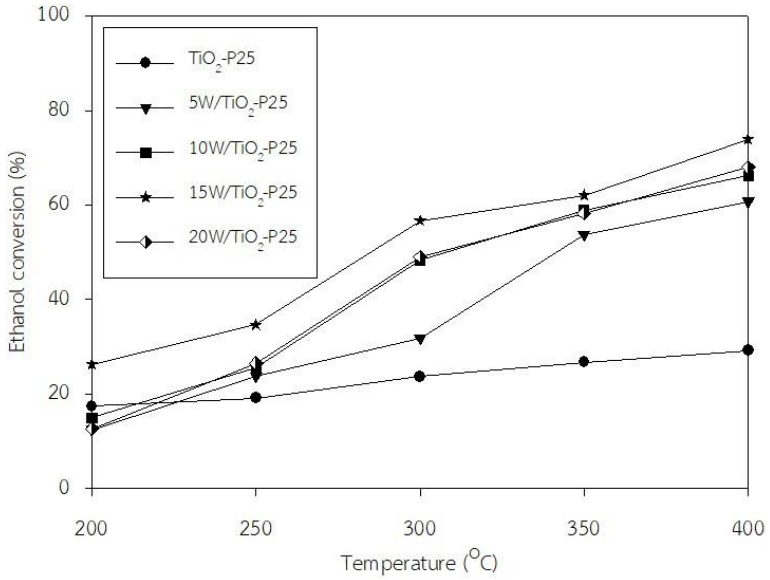

Figure 33 Ethanol conversion of W/TiO_2-P25 catalysts with different W loading

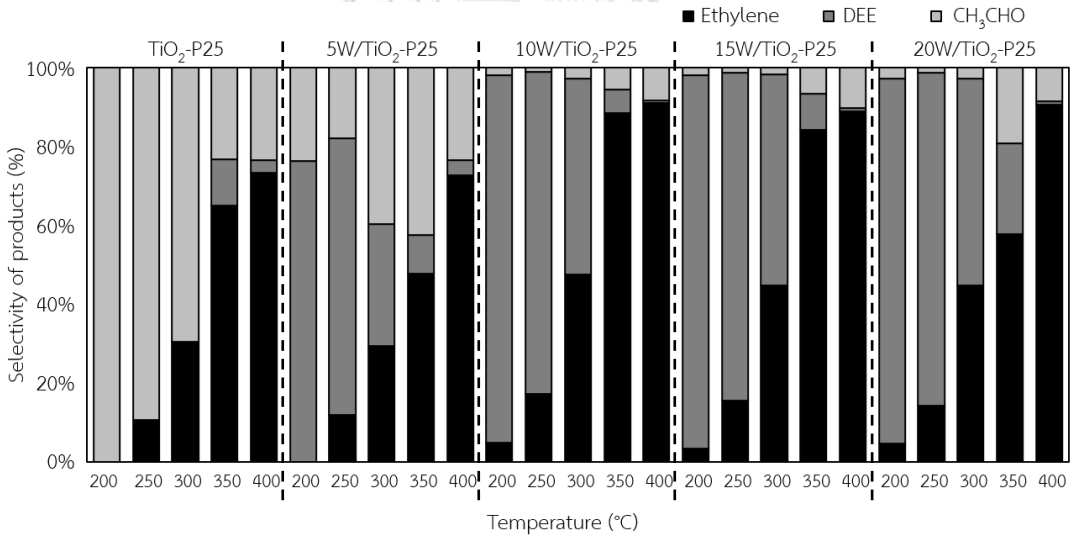

Figure 34 Product selectivities of W/TiO_2 catalysts with different W loading

The selectivity of these TiO_2-P25 support and W/TiO_2-P25 catalysts is exhibited in **Figure 34** as shown above. It can be seen from **Figure 34** that diethyl ether selectivity decreased, whereas ethylene selectivity increased with increasing the reaction temperature. At the reaction temperature above 300°C, diethyl ether is decomposed to ethylene. In addition, increasing W loading over 10 wt% can be slightly changed product selectivities and reduced

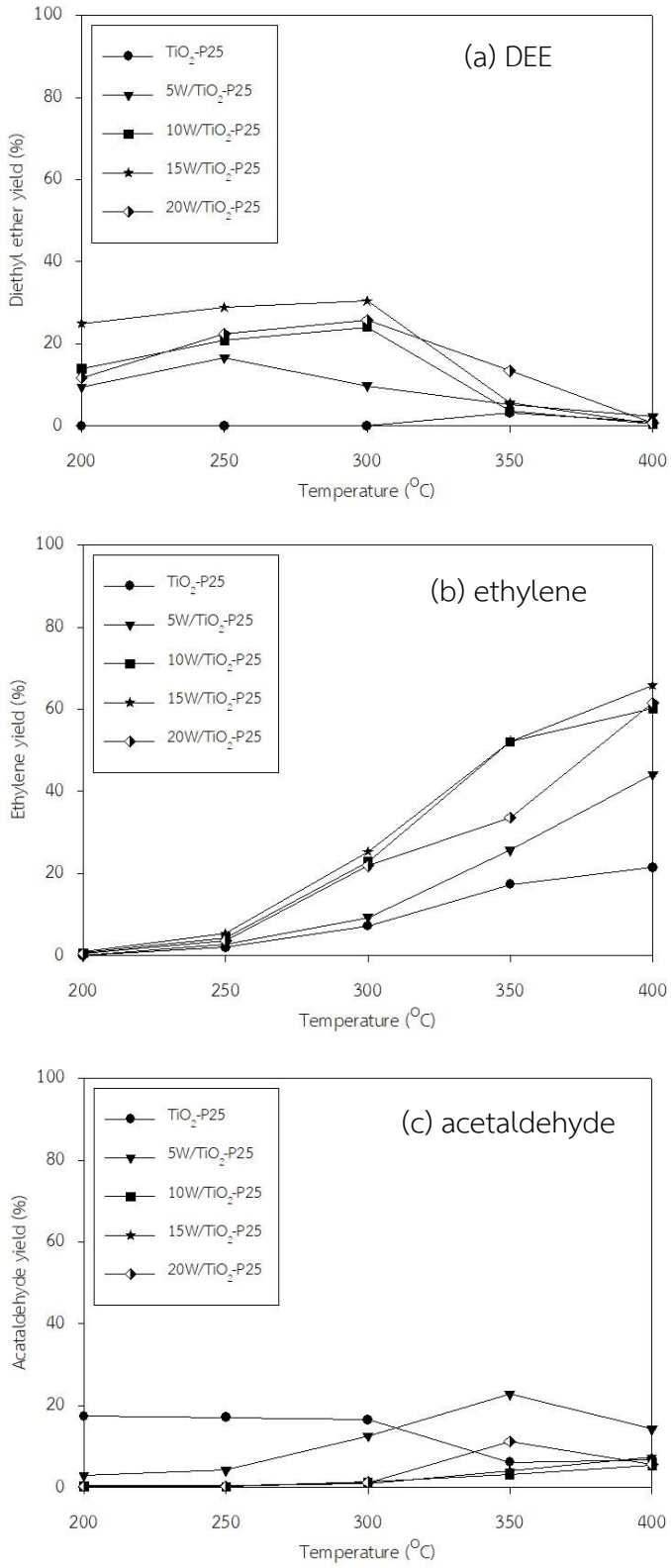

Figure 35 Product yields of TiO_2-P25 support and W/TiO_2-P25 catalysts with different W loading

The product yields of W/TiO_2-P25 catalysts having different W loading are reported in **Figure 35**. Considering for DEE yield as seen in **Figure 35 (a)**, it was observed that the addition of tungsten played roles in increasing DEE yield. At the reaction temperature below 300°C, the addition of tungsten up to 15 wt% increased the DEE yield and gave the highest DEE yield (30.4% at 300°C) for 15W/TiO_2-P25 catalyst.

When consider ethylene yield obtained from these catalysts in **Figure 35 (b)**, it can be found that ethylene yied displayed a similar trend with conversion. This is because the higher temperature gave the higher ethanol conversion and ethylene selectivity. In addition, the highest ethylene selectivity (65.8%) can be obtained from 15W/TiO_2-P25 catalyst at 400°C due to the acidity. Moreover, acetaldehyde was prevented to form as a byproduct by having tungsten deposition as seen in **Figure 35 (c)**.

The summary of all catalytic activities including ethanol conversion, product selectivities and product yields is displayed in **Table 14**. According to the results from this study, it can be seen that the addition of tungsten onto TiO_2-P25 support can affect the catalytic behavior of W/TiO_2-P25 catalysts. 15W/TiO_2-P25 catalyst is more suitable to produce both DEE and ethylene at 300°C and 400°C, respectively.

Table 14 Ethanol conversion, product selectivities and product yields

Catalyst	Temperature (°C)	Ethanol Conversion (%)	Product Selectivity (%)			Product Yield (%)		
			Ethylene	DEE	CH_3CHO	Ethylene	DEE	CH_3CHO
TiO_2-P25	200	17.4	0.0	0.0	100.0	0.0	0.0	17.4
	250	19.2	10.6	0.0	89.4	2.0	0.0	17.2
	300	23.7	30.3	0.0	69.7	7.2	0.0	16.5
	350	26.8	65.0	11.8	23.2	17.4	3.2	6.2
	400	29.3	73.3	3.3	23.4	21.5	1.0	6.8
5W/TiO_2-P25	200	12.5	0.0	76.3	23.7	0.0	9.5	2.9
	250	23.8	11.8	70.2	18.0	2.8	16.7	4.3
	300	31.8	29.4	30.8	39.7	9.4	9.8	12.7
	350	53.8	47.8	9.8	42.4	25.7	5.3	22.8
	400	60.8	72.6	3.9	23.5	44.2	2.3	14.3
10W/TiO_2-P25	200	15.0	4.7	93.4	1.9	0.7	14.0	0.3
	250	25.5	17.1	81.8	1.1	4.4	20.9	0.3
	300	48.3	47.4	49.8	2.7	22.9	24.1	1.3
	350	58.9	88.5	6.1	5.4	52.1	3.6	3.2
	400	66.2	91.1	0.7	8.2	60.3	0.4	5.4
15W/TiO_2-P25	200	26.3	3.3	94.8	1.8	0.9	25.0	0.5
	250	34.6	15.5	83.2	1.2	5.4	28.8	0.4
	300	56.7	44.6	53.6	1.8	25.3	30.4	1.0
	350	62.1	84.1	9.2	6.7	52.3	5.7	4.2
	400	73.9	89.0	0.9	10.1	65.8	0.6	7.5
20W/TiO_2-P25	200	12.7	4.7	92.7	2.7	0.6	11.7	0.3
	250	26.6	14.2	84.5	1.3	3.8	22.5	0.3
	300	49.0	44.8	52.6	2.7	21.9	25.8	1.3
	350	58.3	57.7	23.0	19.3	33.6	13.4	11.2
	400	68.0	90.5	1.0	8.4	61.5	0.7	5.7

4.2.7 Thermal gravimetric analysis (TGA)

To determine the coke formation, the spent catalysts were analyzed by using thermal gravimetric analysis (TGA) as shown in **Figure 36**. It can be seen that TGA curves of all spent catalysts using in the reaction exhibited similar activity.

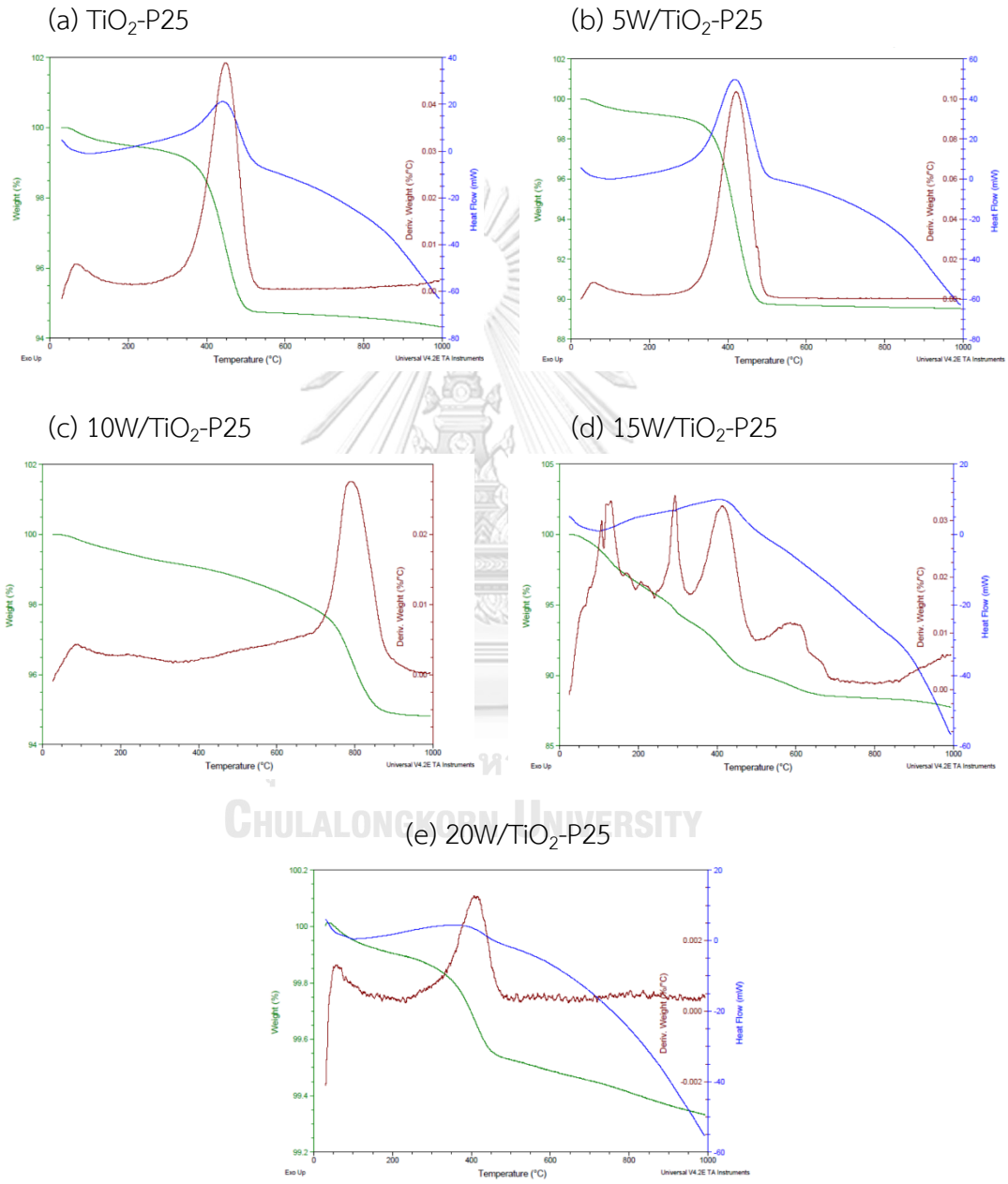

Figure 36 TGA analysis curves of spent catalysts

At temperature higher that 200°C, it was found that the addition of tungsten into TiO_2-P25 catalysts promoted the coke formation due to the catalyst burning. The amount of coke formation in spent catalysts was determined and reported in **Table 15** as follows;

Table 15 The amount of coke formation in the spent catalysts

Catalyst	Temperature (°C)	Weight (%)	The amount of coke formation (%)
TiO_2-P25	200	99.91	0.58
	1000	99.33	
5W/TiO_2-P25	200	99.5	5.20
	1000	94.33	
10W/TiO_2-P25	200	99.51	4.71
	1000	94.82	
15W/TiO_2-P25	200	96.54	9.09
	1000	87.76	
20W/TiO_2-P25	200	99.27	9.80
	1000	89.54	

4.2.8 Catalyst appearance

After modified TiO_2-P25 support with different W loading (0-20 wt%), the obtained W/TiO_2-P25 catalysts were taken to observe the appearance before and after being used in ethanol dehydration reaction. The appearance of fresh and spent W/TiO_2-P25 with different loading of W was presented in **Figure 37** and **Figure 38**, respectively.

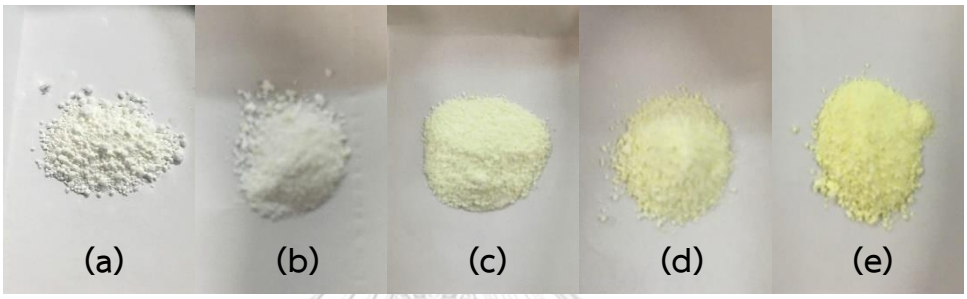

Figure 37 The appearance of fresh W/TiO_2-P25 catalysts
(a) TiO_2-P25 (b) 5W/TiO_2-P25 (c) 10W/TiO_2-P25 (d) 15W/TiO_2-P25 (e) 20W/TiO_2-P25

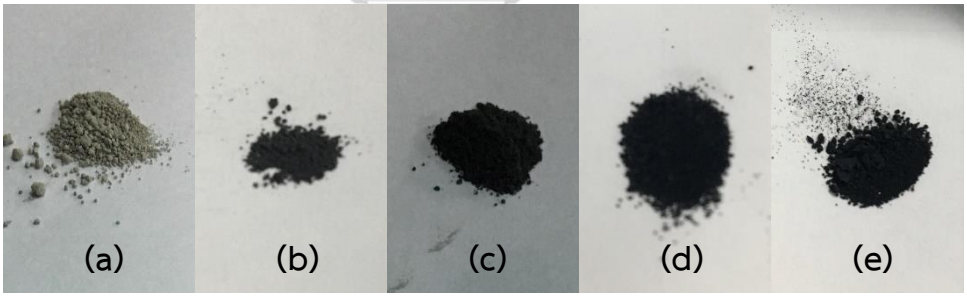

Figure 38 The appearance of spent W/TiO_2-P25 catalysts
(a) TiO_2-P25 (b) 5W/TiO_2-P25 (c) 10W/TiO_2-P25 (d) 15W/TiO_2-P25 (e) 20W/TiO_2-P25

The images of fresh W/TiO_2-P25 catalysts showed that the addition of tungsten led catalysts to have more yellow color indicating the different structure of catalyst, which confirms in previous characterized results. After all catalysts were performed in ethanol dehydration reaction, the spent catalysts in all loading were observed the coke formation on catalysts surface as observed by a change to black color.

Part III : The comparison of catalysts for diethyl ether synthesis and their catalytic activity

Table 16 Comparison of catalysts for DEE synthesis and their catalytic activity

Catalyst	Surface area (m^2/g)	Reaction temperature (°C)	Ethanol conversion (%)	DEE yield (%)	Ref.
$10W/TiO_2$-A	58	200-300	4-40	9-23	This study
$10W/TiO_2$-R	7	200-300	2-22	0-11	This study
$5W/TiO_2$-P25	51	200-300	13-32	10-17	This study
$10W/TiO_2$-P25	53	200-300	15-48	14-24	This study
$15W/TiO_2$-P25	56	200-300	26-57	25-30	This study
$20W/TiO_2$-P25	46	200-300	13-49	12-26	This study
HBZ	522	250	66	35	[5]
Ru-HBZ	541	250	73	47	[5]
Pt-HBZ	561	250	70	45	[5]
WO_3/ZrO_2	81	200-300	9-98	8-42	[10]
WO_3/TiO_2 (H)	60	200-300	70-100	1-68	[10]
H-ZSM-5	366	300	90	14	[45]
20HP-ZSM-5	74	250-450	25-100	0-24	[45]

The catalytic activity for ethanol dehydration to diethyl ether over various catalysts were summarized in **Table 16**. It is displayed that W/TiO_2 catalysts in this study are comparable to other catalysts. Form the catalytic activity of HBZ, modified HBZ, WO_3/ZrO_2 and WO_3/TiO_2 catalysts for ethanol dehydration, it was found that these catalysts were much higher surface area that of W/TiO_2 catalyst for this study. Then, the result showed that ethanol conversion and DEE yield were higher than catalysts in this study. On the other hand, H-ZSM-5 and 20HP-ZSM-5 catalysts were lower surface area than $15W/TiO_2$-P25 catalyst resulting lower DEE yield. Thus, $15W/TiO_2$-P25 catalysts is an alternative route to obtain DEE via ethanol dehydration.

CHAPTER 5
CONCLUSIONS AND RECOMMENDATIONS

In this study, the results of TiO_2 supports having three different phases (anatase, rutile and mixed phases) and W/TiO_2-P25 catalysts having W loading (0-20 wt%) are considered to charateristics and catalytic performance via ethanol dehydration reaction. Therefore, the research conclusions and reccomendations are explained in **section 5.1** and **section 5.2**, respectively.

5.1 Conclusions

1. The W/TiO_2 catalysts having three different phases of anatase (A), rutile (R) and mixed phases (P25) in titania supports can be employed for catalytic ethanol dehydration to ethylene and DEE.

2. The highest activity obtained from the 10W/TiO_2-P25 catalyst can be attributed to highest surface area and largest amount of W species distribution on the external surface of catalyst.

3. The three different phases of titania supports have the effect on the characteristics , which are all explained as follows;

- The BET surface area and pore volume of both TiO_2-A and TiO_2-P25 supports are higher than those of TiO_2-R support. The addition of 10 wt% tungsten onto titania supports slightly changed the textural properties.
- The acid sites of catalysts do not have a significant difference.

4. TiO_2-P25 support is more suitable support than both of TiO_2-A and TiO_2-R supports. It reveals that 10W/TiO_2-P25 catalyst is able to produce DEE (24.1% yield) at 300°C and ethylene (60.3% yield) at 400°C.

5. The different tungsten loading has the effect on characteristics , which are all explained as follows;

- The addition of tungsten up to 15 wt% slightly increases BET surface area. For the further addition of tungsten, the textural properties tend to decrease.

- The acid sites of catalysts slightly increase with increasing tungsten loading up to 15 wt% W.

5. 15W/TiO_2-P25 catalyst gives the highest DEE yield of 30.4% at 300°C and ethylene yield of 65.8% at 400°C.

6. The mixed phases (P25) of anatase and rutile titania are more suitable for W probably due to its three major roles including; (1) high surface area, (2) high amount of W species distributed on the external surface of catalyst and (3) introduce acid sites as active sites in the reaction. There were the factors leading to obtain higher activity for ethanol dehydration of 15W/TiO_2-P25 catalyst.

5.2 Recommendations

1. The acidity is strongly important for ethanol dehydration reaction. Types of acid, both Lewis and Brønsted acid sites, should be measured by using pyridine adsorption analysis.

2. The catalytic stability of 15W/TiO_2-P25 catalyst should be further investigated.

3. The preparation of mixed phases of TiO_2 support should be studied to obtain the optimum phase composition of TiO_2 support.

REFERENCES

1. Sebayang, A.H., et al., *A perspective on bioethanol production from biomass as alternative fuel for spark ignition engine.* RSC Advances, 2016. **6**(18): p. 14964-14992.
2. Phung, T.K., et al., *Dehydration of ethanol over zeolites, silica alumina and alumina: Lewis acidity, Brønsted acidity and confinement effects.* Applied Catalysis A: General, 2015. **493**: p. 77-89.
3. Soh, J.C., et al., *Catalytic ethylene production from ethanol dehydration over non-modified and phosphoric acid modified Zeolite H-Y (80) catalysts.* Fuel Processing Technology, 2017. **158**: p. 85-95.
4. Alharbi, W., et al., *Dehydration of ethanol over heteropoly acid catalysts in the gas phase.* Journal of Catalysis, 2014. **319**: p. 174-181.
5. Kamsuwan, T., P. Praserthdam, and B. Jongsomjit, *Diethyl Ether Production during Catalytic Dehydration of Ethanol over Ru- and Pt- modified H-beta Zeolite Catalysts.* Journal of Oleo Science, 2016. **66**(2): p. 199-207.
6. Phung, T.K. and G. Busca, *Diethyl ether cracking and ethanol dehydration: Acid catalysis and reaction paths.* Chemical Engineering Journal, 2015. **272**: p. 92-101.
7. Chen, B., et al., *Dehydration of bio-ethanol to ethylene over iron exchanged HZSM-5.* Chinese Journal of Catalysis, 2016. **37**(11): p. 1941-1948.
8. Lee, J., J. Szanyi, and J.H. Kwak, *Ethanol dehydration on γ-Al_2O_3: Effects of partial pressure and temperature.* Molecular Catalysis, 2017. **434**: p. 39-48.
9. Thomas Onfroy, G.C., Saeed B. Bukallah, Tom Visser, Marwan Houalla, *Acidity of titania-supported tungsten or niobium oxide catalysts Correlation with catalytic activity.* Applied Catalysis A: General, 2006. **298**: p. 80-87.
10. Phung, T.K., L. Proietti Hernández, and G. Busca, *Conversion of ethanol over transition metal oxide catalysts: Effect of tungsta addition on catalytic*

behaviour of titania and zirconia. Applied Catalysis A: General, 2015. **489**: p. 180-187.

11. Jongsomjit, B., T. Wongsalee, and P. Praserthdam, *Characteristics and catalytic properties of Co/TiO_2 for various rutile:anatase ratios.* Catalysis Communications, 2005. **6**(11): p. 705-710.
12. Jongsomjit, B., T. Wongsalee, and P. Praserthdam, *Study of cobalt dispersion on titania consisting various rutile:anatase ratios.* Materials Chemistry and Physics, 2005. **92**(2): p. 572-577.
13. Kordouli, E., et al., *Comparative study of phase transition and textural changes upon calcination of two commercial titania samples: A pure anatase and a mixed anatase-rutile.* Journal of Solid State Chemistry, 2015. **232**: p. 42-49.
14. Amores, M.J., et al., *Life cycle assessment of fuel ethanol from sugarcane in Argentina.* The International Journal of Life Cycle Assessment, 2013. **18**(7): p. 1344-1357.
15. Mizuno, N. and M. Misono, *Heterogeneous Catalysis.* Chemical Reviews, 1998. **98**(1): p. 199-218.
16. DeWilde, J.F., C.J. Czopinski, and A. Bhan, *Ethanol Dehydration and Dehydrogenation on γ-Al_2O_3: Mechanism of Acetaldehyde Formation.* ACS Catalysis, 2014. **4**(12): p. 4425-4433.
17. Li, Z., et al., *Alcohol Dehydration on Monooxo W═O and Dioxo O═W═O Species.* The Journal of Physical Chemistry Letters, 2012. **3**(16): p. 2168-2172.
18. Pokhrel, S., et al., *In situ high temperature X-ray diffraction, transmission electron microscopy and theoretical modeling for the formation of WO_3 crystallites.* Cryst Eng Comm, 2015. **17**(36): p. 6985-6998.
19. Al-Kandari, H., et al., *Creation of surface catalytic active sites on tungsten oxide(s) and a study of the catalytic behavior in isopropanol and 1-hexene reactions.* Reaction Kinetics, Mechanisms and Catalysis, 2017. **122**(1): p. 513-523.
20. AZoM. *Titanium Dioxide - Titania (TiO2)*. 2002; Available from: https://www.azom.com/article.aspx?ArticleID=1179#.

21. Pimenta, S., et al., *Design and fabrication of SiO_2/TiO_2 and MgO/TiO_2 based high selective optical filters for diffuse reflectance and fluorescence signals extraction.* Biomedical Optics Express, 2015. **6**(8): p. 3084-3098.

22. Hamdan, H., *Fabrication of TiO_2 Nanotubes Using Electrochemical Anodization Republic of Iraq Fabrication of TiO_2 Nanotubes Using Electrochemical Anodization Supervised by*. 2012.

23. Wagner, T., et al., *Mesoporous materials as gas sensors.* Chemical Society Reviews, 2013. **42**(9): p. 4036-4053.

24. Average, B. *Your mom is like a heterogeneous catalyst solid support*. 2013; Available from: https://yourmomislike.wordpress.com/2013/02/17/your-mom-is-like-a-heterogeneous-catalyst-solid-support/.

25. Janlamool, J. and B. Jongsomjit, *Oxidative dehydrogenation of ethanol over AgLi–Al_2O_3 catalysts containing different phases of alumina.* Catalysis Communications, 2015. **70**: p. 49-52.

26. Krutpijit, C. and B. Jongsomjit, *Effect of HCl Loading and Ethanol Concentration over HCl-Activated Clay Catalysts for Ethanol Dehydration to Ethylene.* Journal of Oleo Science, 2017. **66**(12): p. 1355-1364.

27. Autthanit, C. and B. Jongsomjit, *Production of Ethylene through Ethanol Dehydration on SBA-15 Catalysts Synthesized by Sol-gel and One-step Hydrothermal Methods.* Journal of oleo science, 2018. **67**(2): p. 235-243.

28. Chanchuey, T., C. Autthanit, and B. Jongsomjit, *Effect of Mo-Doped Mesoporous Al-SSP Catalysts for the Catalytic Dehydration of Ethanol to Ethylene.* Journal of Chemistry, 2016. **2016**: p. 8.

29. Krutpijit, C. and B. Jongsomjit, *Catalytic Ethanol Dehydration over Different Acid-activated Montmorillonite Clays.* Journal of Oleo Science, 2016. **65**(4): p. 347-355.

30. Said, A.E.-A.A., M.M.M.A. El-Wahab, and M.M. Abdelhak, *The role of Brønsted acid site strength on the catalytic performance of phosphotungstic acid supported on nano c-alumina catalysts for the dehydration of ethanol to diethyl ether.* Reaction Kinetics, Mechanisms and Catalysis, 2017: p. 1-17.

31. de Oliveira, T.K.R., M. Rosset, and O.W. Perez-Lopez, *Ethanol dehydration to diethyl ether over Cu-Fe/ZSM-5 catalysts.* Catalysis Communications, 2018. **104**: p. 32-36.

32. Kamsuwan, T. and B. Jongsomjit, *A Comparative Study of Different Al-based Solid Acid Catalysts for Catalytic Dehydration of Ethanol.* 2016.

33. He, Y., et al., *Selective catalytic reduction of NO by NH_3 with WO_3-TiO_2 catalysts: Influence of catalyst synthesis method.* Applied Catalysis B: Environmental, 2016. **188**: p. 123-133.

34. Xu, H., et al., *Tuning the morphology, stability and photocatalytic activity of TiO_2 nanocrystal colloids by tungsten doping.* Materials Research Bulletin, 2014. **51**: p. 326-331.

35. Panagiotou, G.D., et al., *The interfacial chemistry of the impregnation step involved in the preparation of tungsten(VI) supported titania catalysts.* Journal of Catalysis, 2009. **262**(2): p. 266-279.

36. Ladera, R., et al., *Supported WO_x-based catalysts for methanol dehydration to dimethyl ether.* Fuel, 2013. **113**: p. 1-9.

37. Onfroy, T., et al., *Quantitative relationship between the nature of surface species and the catalytic activity of tungsten oxides supported on crystallized titania.* Journal of Molecular Catalysis A: Chemical, 2010. **318**(1): p. 1-7.

38. Sohn, J.R. and J.H. Bae, *Characterization of tungsten oxide supported on TiO_2 and activity for acid catalysis.* Korean Journal of Chemical Engineering, 2000. **17**(1): p. 86-92.

39. Rodriguez, J.A. and D. Stacchiola, *Catalysis and the nature of mixed-metal oxides at the nanometer level: special properties of $MO_x/TiO_2(110)$ {M= V, W, Ce} surfaces.* Physical Chemistry Chemical Physics, 2010. **12**(33): p. 9557-9565.

40. Kolen'ko, Y.V., et al., *Synthesis of nanocrystalline TiO_2 powders from aqueous $TiOSO_4$ solutions under hydrothermal conditions.* Materials Letters, 2003. **57**(5): p. 1124-1129.

41. Zhang, H., H. Bian, and S. Zhang, *Study on the catalytic activity of vanadium doped TiO_2: Anatase-to-rutile phase transition.* Russian Journal of Physical Chemistry A, 2016. **90**(1): p. 60-64.

42. Yao, X., et al., *Selective catalytic reduction of NO_x by NH_3 over CeO_2 supported on TiO_2: Comparison of anatase, brookite, and rutile.* Applied Catalysis B: Environmental, 2017. **208**: p. 82-93.

43. Rui, Z., et al., *Comparison of TiO_2 Degussa P25 with anatase and rutile crystalline phases for methane combustion.* Chemical Engineering Journal, 2014. **243**: p. 254-264.

44. Raj, K.J.A. and B. Viswanathan, *Effect of surface area, pore volume and particle size of P25 titania on the phase transformation of anatase to rutile.* Indian Journal of Chemistry, 2009. **48A**: p. 1378-1382.

45. Ramesh, K., et al., *Structure and reactivity of phosphorous modified H-ZSM-5 catalysts for ethanol dehydration.* Catalysis communications, 2009. **10**: p. 567-571.

APPENDIX

APPENDIX A

CALCULATION FOR CATALYST PREPARATION

Calculation for preparation of 10W/TiO_2 catalysts having different phase of TiO_2

1. Impregnated of 10 wt% W onto three different TiO_2 supports

Catalyst: - Ammonium metatungstate ($(NH_4)_6H_2W_{12}O_{40} \cdot 4H_2O$)

Molecular weight = 3028.36 g/mol

Tungsten (W) weight = 183.84 x 12 = 2206.08 g/mol

Support: - Titania (TiO_2) supports: anatase (A), rutile (R) and mixed phases (P25)

<u>Basis</u> 1 g of catalyst;

10 wt% of tungsten (W) = 0.10 g

TiO_2 support (A, R and P25) = 1.00-0.10 = 0.90 g

There is 2206.08 g of W in 3028.36 g of ammonium metatungstate

Thus, there is 0.10 g of W in 0.10 x 3028.36 / 2206.08

= 0.137 g of ammonium metatungstate

Then, an aqueous precursor solution was mixed with support and then stirred for 30 minutes to obtain non-calcined **10W/TiO_2-A, 10W/TiO_2-R** and **10W/TiO_2-P25** catalysts.

Calculation for preparation of W/TiO_2-P25 catalysts having different W loading

1. Impregnated of 5, 15, 20 wt% W onto TiO_2-P25 support

Catalyst: - Ammonium metatungstate ($(NH_4)_6H_2W_{12}O_{40} \cdot 4H_2O$)

Molecular weight = 3028.36 g/mol

Tungsten (W) weight = 183.84 x 12 = 2206.08 g/mol

- 5, 15, 20 wt% W were selected to study

Support: - TiO_2-P25

<u>Basis</u> 1 g of catalyst;

(1) 5 wt% of tungsten (W) = 0.05 g

TiO_2-P25 support = 1.00-0.05 = 0.95 g

Thus, ammonium metatungstate = 0.05 x 3028.36 / 2206.08 = 0.069 g

(2) 15 wt% of tungsten (W) = 0.15 g

TiO_2-P25 support = 1.00-0.15 = 0.85 g

Thus, ammonium metatungstate = 0.15 x 3028.36 / 2206.08 = 0.206 g

(3) 20 wt% of tungsten (W) = 0.20 g

TiO_2-P25 support = 1.00-0.20 = 0.80 g

Thus, ammonium metatungstate = 0.20 x 3028.36 / 2206.08 = 0.275 g

Then, an aqueous precursor solution was mixed with support and then stirred for 30 minutes to obtain non-calcined **5W/TiO_2-P25, 15W/TiO_2-P25** and **20W/TiO_2-P25** catalysts, respectively.

APPENDIX B

CALCULATION FOR ACIDITY

The acidity of all supports and catalysts is determined from NH3-TPD by calculating the area under TCD signal versus temperature.

$$\text{Acidity of catalysts} = \frac{\text{mol of desorbed } NH_3}{\text{weight of dry catalyst}} \quad [\mu\text{mol/g cat}]$$

Where mol of desorbed NH_3 = (area under TCD signal curve) x (30.927 μmol)

weight of dry catalyst = 0.05 g

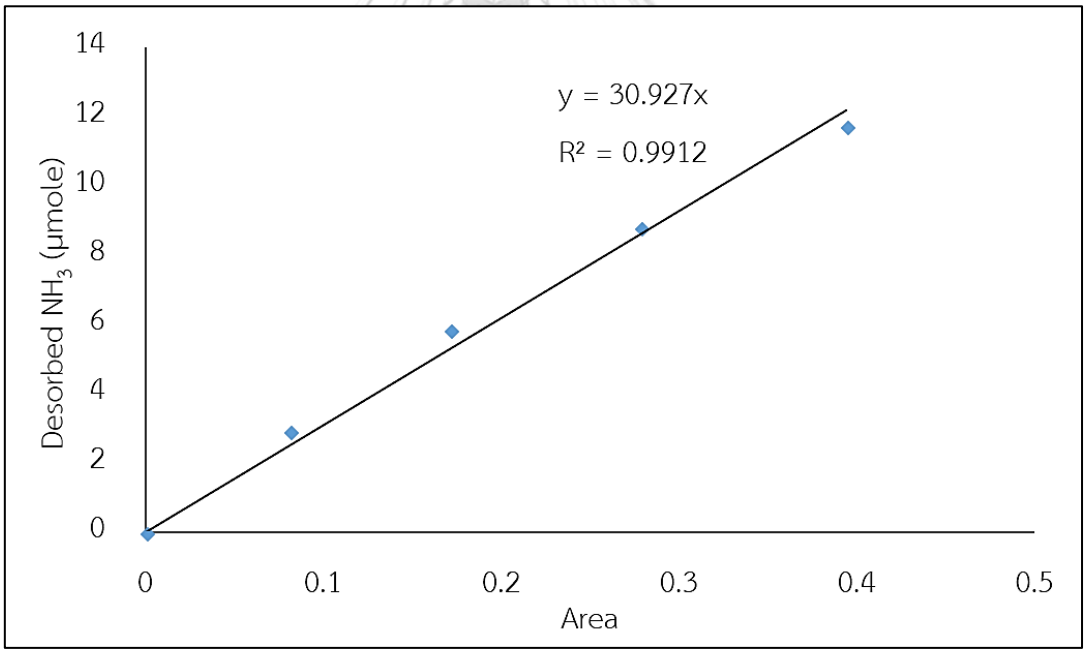

Figure B.1 The calibration curve of NH_3-TPD

APPENDIX C

CALIBRATION CURVES OF REACTANT AND PRODUCTS

The calibration curves of reactant and products were used to calculate the amount of reactant and products including ethanol, ethylene, diethyl ether and acetaldehyde as showed in **Figure C.1-C.4**.

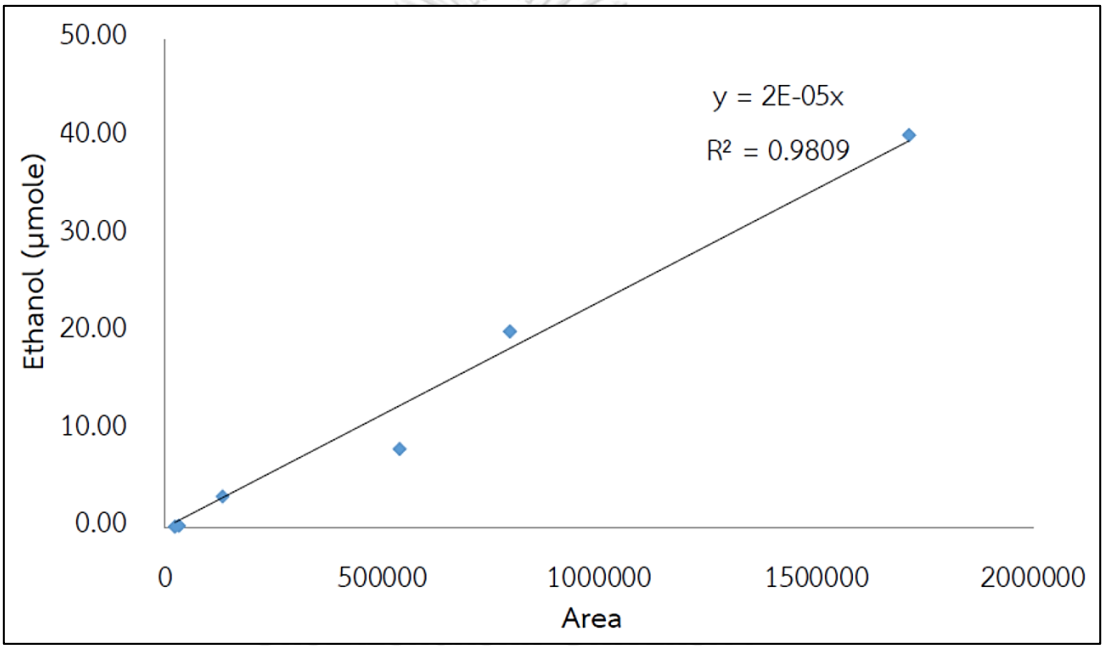

Figure C.1 The calibration curve of ethanol

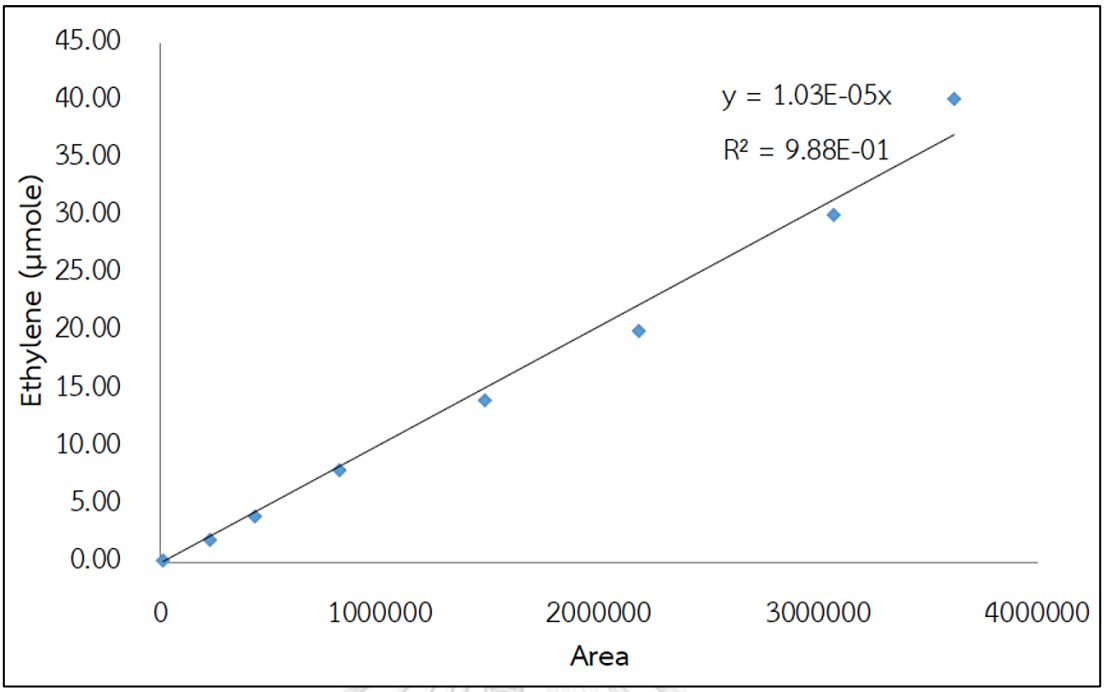

Figure C.2 The calibration curve of ethylene

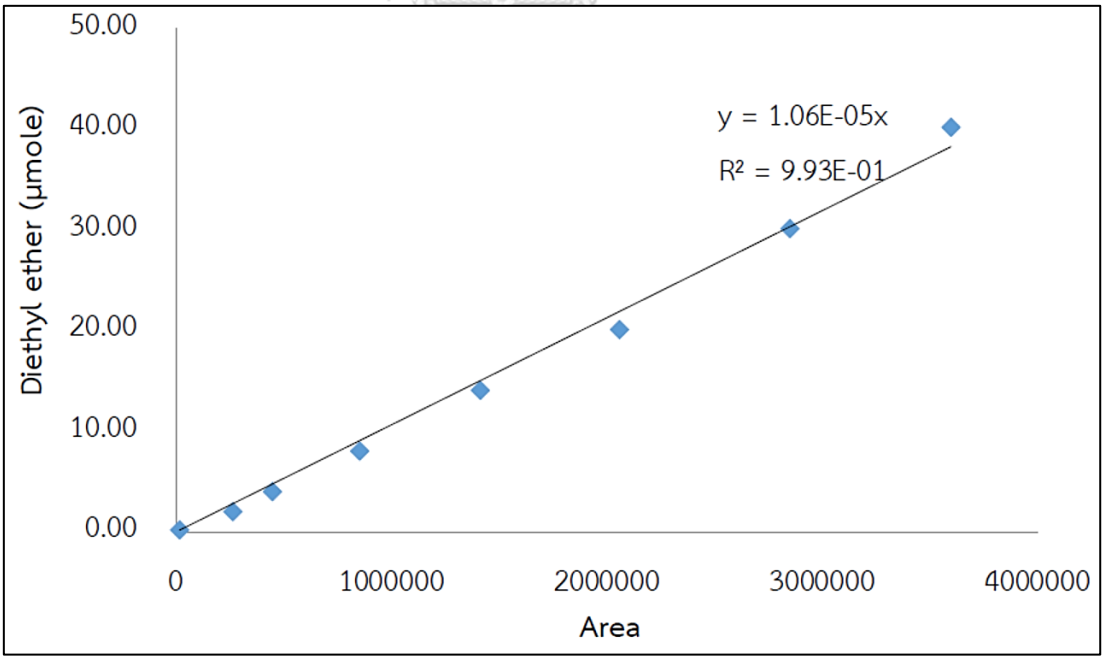

Figure C.3 The calibration curve of diethyl ether

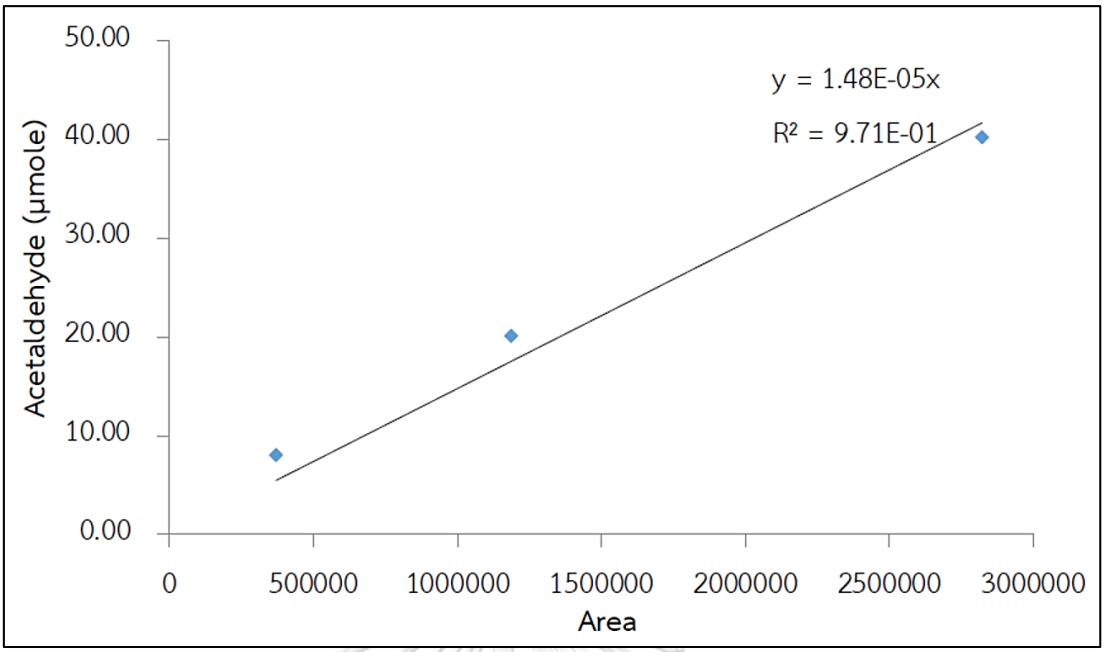

Figure C.4 The calibration curve of acetaldehyde

APPENDIX D

CHROMATOGRAM

The peak positions of reactant and products showed as below;

Reactant:	ethanol peak position	= 4.9 min
Products:	ethylene peak position	= 4.4 min
	diethyl ether peak position	= 5.2 min
	acetaldehyde peak position	= 4.6 min

APPENDIX E

CONVERSION, SELECTTIVITY AND YIELD

The catalytic activities (conversion, selectivity and yield) were calculated as follows;

1. Ethanol conversion

$$\text{Ethanol conversion (\%)} = \frac{\text{(mol of ethanol in feed - mol of ethanol in product)}}{\text{mol of ethanol in feed}} \times 100$$

2. Product selectivity

$$\text{Product selectivity (\%)} = \frac{\text{mol of each product}}{\text{mol of total products}} \times 100$$

3. Product yield

$$\text{Product yield (\%)} = \frac{\text{ethanol conversion x selectivity of each product}}{100}$$

APPENDIX F
LIST OF PUBLICATION

Proceeding

Pongsatorn Kerdnoi, Theerut Kositanont, Teerotorn Vipattipumiprathet, Nithinart Chitpong and Bunjerd Jongsomjit, "CATALYTIC DEHYDRATION OF ETHANOL OVER W/TIO_2 CATALYSTS HAVING DIFFERENT PHASES OF TITANIA"
Proceeding of the 7th International TIChE Conference (ITIChE2017) "Innovative Chemical Engineering and Technology toward Sustainable Future", Shangri-La Hotel, Bangkok, Thailand, October 18-20, 2017.

VITA

Mr. Pongsatorn Kerdnoi was born on November 30th, 1991 in Nonthaburi, Thailand. He finished high school from Pakkred Secondary School in 2009 and received the bachelor's degree from Department of Chemical Technology, Faculty of Science, Chulalongkorn University in 2015. He has continued his study in the master's degree at Department of Chemical Engineering, Faculty of Engineering, Chulalongkorn University in 2017.